Supplementary Materials and Methods

Genetically engineered mutant IDH1 glioma model

The wild type (WT)-IDH1 and mIDH1 glioma models used in this study were generated previously for our group using SB Transposon System.[15] The plasmid used to generate those models are: (i) SB transposase and LUC (pT2C-LucPGK-SB100X, henceforth referred to as SB/Luc), (ii) a constitutively active mutant of NRAS, NRAS-G12V (pT2CAG-NRASV12, henceforth referred to as NRAS), (iii) a short hairpin against p53 (pT2-shp53-GFP4, henceforth referred to as shp53), (iv) a short hairpin against ATRX (pT2-shATRX53-GFP4, henceforth referred to as shATRX), and (v) mutant $IDH1^{R132H}$ (pKT-$IDH1^{R132H}$-IRES-Katushka, henceforth referred to as mIDH1). Neonatal P01 C57BL/6 mice were used in all experiments. The genotype of SB- generated mice involved these combinations: (i) NRAS, shP53, and shATRX (WT-IDH1) and (ii) NRAS, shp53, shATRX, and $IDH1^{R132H}$ (mIDH1). Mice were injected according to a previously described protocol [78]. Plasmids were mixed in mass ratios of 1:2:2:2 or 1:2:2:2:2 (20 μg plasmid in a total of 40 μL plasmid mixture) with in vivo-jetPEI (Polyplus Transfection, 201-50G) (2.8 μL per 40 μL plasmid mixture) and dextrose (5% total) and maintained at room temperature for at least 15 min prior to injection. The lateral ventricle (1.5 mm AP, 0.7 mm lateral, and 1.5 mm deep from lambda) of neonatal mice (P01) was injected with 0.75 μL plasmid mixture (0.5 μL/min) that included: (1) SB/Luc, (2) NRAS, (3) shp53, (4) with or without shATRX, and (5) with or without $IDH1^{R132H}$. To monitor plasmid uptake in neonatal pups, 30 μL of luciferin (30 mg/mL) was injected s.c. into each pup 24-48h after plasmid injection. In vivo bioluminescence was measured on an IVIS Spectrum (Perkin Elmer, 124262) imaging system. For the IVIS spectrum, the following settings were used: automatic exposure, large binning, and aperture f=1. For in vivo imaging of tumor formation and progression in adult mice, 100 μL of luciferin solution was injected i.p. and mice were then anesthetized with oxygen/isoflurane (1.5-2.5% isoflurane). To score luminescence, Living

Image Software Version 4.3.1 (Caliper Life Sciences) was used. A region of interest (ROI) was defined as a circle over the head, and luminescence intensity was measured using the calibrated unit's photons/s/cm2/sr. Multiple images were taken over a 25min period following injection, and maximal intensity was reported.

For survival studies, animals were monitored daily for signs of morbidity, including ataxia, impaired mobility, hunched posture, seizures, and scruffy fur. Animals displaying symptoms of morbidity were intracardially perfused using Tyrode's solution, followed by fixation with 4% paraformaldehyde (PFA) in PBS.

Alternative genetically engineered mouse glioma models

In CPA/CPAI models, the genetic lesions were incorporated into neonatal CDKN2A homozygous knocked-down ($CDKN2A^{-/-}$) mice.[12] $CDKN2A^{-/-}$ mice were obtained from the Frederick National Library for Cancer Research as frozen embryos. Embryos were implanted into receptive adult B6 females by the Transgenic Animal Core of the University of Michigan and the obtained transgenic mice, which were CDKN2A heterozygous, were mated with B6 mice. The CDKN2A KO heterozygous mice of second generation were mated and the progeny obtained was genotyped to confirm the homozygous CDKN2A deletion. From this point, the $CDKN2A^{-/-}$ colony was maintained by mating $CDKN2A^{-/-}$ mice and monitored regularly by CDKN2A genotypification. The genotype of the genetically engineered mice involved these combinations: (i) CDKN2A deletion, TP53 and ATRX short hairpin knockdown, with or without IDH1-R132H. In the RPA/RPAI models, glioma was driven by platelet derived growth factor receptor alpha mutation ($PDGFRA^{D842V}$) to promote constituent activation of the MAPK pathway.[18] These mouse glioma cells include ATRX and TP53 short hairpin knockdown, with or without endogenous express IDH1-R132H, to simulate the molecular genetic lesions that define the molecular features of astrocytoma.

Primary glioma neurosphere cultures (NS)

Mouse glioma neurosphere (NS) cultures were generated as previously described.[15,79] Briefly, brain tumors in mice were harvested at the time of euthanasia by intracardial perfusion with Tyrode's solution only. The tumor mass was dissociated using non-enzymatic cell dissociation buffer, filtered through a 70 µm strainer and maintained in neural stem cell medium DMEM/F12 with L-Glutamine (Gibco, 11320-033), B-27 supplement without Vitamin A (1X) (Gibco, 12587-010), N-2 supplement (1X) (Gibco, 17502-048), Penicillin-Streptomycin (100X) (10,000 IU Penicillin) (10,000 µg/mL Streptomycin) (Corning, Cellgro, 30-001-CI), and Normocin (1X) (Invivogen, ant-nr-1) at 37°C, 5% CO_2. Human-EGF (Peprotech, 100-15) and human-FGF (Peprotech, 100-18) were added twice weekly at 1 µL (20 ng/µL each stock) per 1 mL medium for a final concentration of 20 ng/mL. For reduced growth conditions, human-EGF and human-FGF were added twice weekly at 1 µL (20 ng/µL) per 3 mL medium for a final concentration of 6.6 ng/mL.

RNA-seq and bioinformatics analysis

RNA-seq was performed in collaboration with the University of Michigan sequencing core. All the RNA-seq datasets used to identify differential enrichments related with metabolism and autophagy were previously generated in our lab[15] with public access. Briefly, RNA was isolated from tumor NS and 100 ng samples of purified RNA were sent for RNA Seq analysis. After passing all quality controls, Illumina HiSeq 2500/4000 fastq files were processed using the Tuxedo Suite for alignment and differential expression analysis. Genes and transcripts were identified as differentially expressed based on three criteria: test status = "OK", FDR ≤ 0.05, and fold change ≥ ± 1.5 Gene Ontology (GO) enrichment analysis, which was performed using iPathwayGuide (http://www.advaitabio.com/ipathwayguide) separately for upregulated and downregulated genes. GO Biological Processes, selected for relevance to phenotype, were plotted in a horizontal bar graph using R. Gene set analysis (GSA) was performed using the R package GSA (http://statweb.stanford.edu/~tibs/GSA/), which

implements a version of Gene Set Enrichment Analysis (GSEA)[80] with improved power statistics.[81] GSA takes an expression matrix and a gene set collection as input. The Gene Set Knowledgebase (GSKB) data package (version 1.3.0) was downloaded from Bioconductor. GSKB is specific to mice and includes annotation from over 40 sources. GSA outputs significant gene sets (FDR $\leq$ 0.05), both negatively and positively correlated to phenotype, as well as normalized enrichment scores, and the lists of genes contributing to the significance of each gene set (FDR $\leq$ 0.05). For each list of genes found in a GSKB functional term we tested for enrichment in a small set of Gene Ontology terms, selected for relevance to the phenotype, using the hypergeometric test in R. After RNA-seq analysis, enrichment maps were generated using the Cytoscape platform with enrichment map; the designation of node color was amended to complement our RNA-seq expression color scheme of positively (red) and negatively (green) regulated pathways. The stringency of FDR was reduced to truly encapsulate the underlying biological ramifications of ATRX and IDH1 mutations in our transposon-mediated tumor formation model. Heatmaps were plotted with Heatmap2 package in R. RNA-seq datasets have been deposited in NCBI's Gene Expression Omnibus with identifiers GSE94902, GSE94974, and GSE94975.

Bru-seq and bioinformatics analysis

The Bru-seq dataset used in this work to compare transcriptional levels of genes related with metabolism and autophagy was previously generated as described in.[15] The protocol used was described in.[82] Nascent RNA labeling was performed for 30 min at 37°C with 2 mM 5-bromouridine in conditioned medium. The cells were then incubated for 6h at 37°C. At the completion of labeling, the cells were lysed in TRIzol, and the Bru-containing RNA was isolated using anti-BrdU antibodies conjugated to magnetic beads. The isolated RNA was converted into cDNA libraries and prepared for sequencing using the Illumina TruSeq RNA Library Preparation Kit v2 followed by deep sequencing to around 50 million single-end 50

nucleotide reads. Bioinformatics and data analysis pipeline was implemented using the q pipeline manager (http://sourceforge.net/projects/qppln-mngr/). The bioinformatics programs used, read mapping, genome annotation, and expression scoring were previously described,[82] section 2.4. RPKM (reads per kilobase per million mapped reads) values were calculated for individual genes that were at least 300 bp long. For genes with lengths of 30 kb and less, RPKM values were calculated using read counts from the entire gene. For genes longer than 30 kb, an RPKM value was calculated using read counts from the first 30 kb downstream of the TSS. The R package DESeq35 was used to test differential expression of genes where the mean RPKM between samples was greater than 0.5. Significant changes in transcription initiation were defined as follows: adjusted p-values < 0.05; fold change < 1.5.

ChIP-Sequencing and bioinformatics analysis

For each immunoprecipitation (IP) performed, $1x10^6$ NS were collected, washed in HBSS (Gibco), and pelleted in low binding Corning Costar microtubes. A 95 µL aliquot of digestion buffer (50 mM Tris-HCl (Sigma Aldrich), 1 mM $CaCl_2$ (Sigma Aldrich), 0.2% Triton X-100 (Sigma Aldrich), pH 8.0) supplemented with 1:100 protease inhibitors (Sigma Aldrich) was added per $1x10^6$ NS and immediately pipetted gently up and down to lyse. Chromatin digestion was initiated by the addition of 5 µL of Micrococcal Nuclease (ThermoFisher Scientific at 3.83×10^{-3} U/µL final concentration, for 12 minutes at 37°C, and stopped by the addition of 10X stopping buffer (110 mM Tris-HCl, 55 mM EDTA (Sigma Aldrich), pH 8). The lysate was then diluted with an equal volume of X2 RIPA buffer (280 mM NaCl (Sigma Aldrich), 5 mM EGTA (ThermoFisher Scientific), protease inhibitor diluted 1:100). At this stage 10% of the lysate volume was withdrawn as input. The remaining lysate was then precleared with 10 µL of Dynabeads (1:1 mixture of Protin A (ThermoFisher Scientific) and protein G (ThermoFisher Scientific)) and washed in TIP buffer (10 mM Tris-HCl, 1 mM EDTA, 140 mM NaCl, 1% Triton X-100, 0.1% SDS, 0.1% sodium deoxycholate, pH

8).). Samples were then incubated overnight at 4°C with 1 µg of anti-H3K4me3 (Diagenode, C15410003), anti-H3K27ac antibody (Diagenode), anti-H3K27me3 antibody (Diagenode), anti-H3K36me3 antibody (Diagenode) or anti-total mouse IgG antibody (Santa Cruz Biotech). Antibodies were validated prior to use with Active Mofit's MODified Histone Peptide Array (Active Motif). Immunoprecipitation was performed in the follow day by incubating the samples for 3 hours with 10 µL of Dynabeads (1:1 mixture of Protein A and Protein G (ThermoFisher Scientific)) in 1x RIPA, followed by washing steps with 1x RIPA (5 times, supplemented with 1:1000 dilution of protease inhibitor (Sigma Aldrich)), LiCl buffer (1 time, 250 mM LiCl (Sigma Aldrich, 10 mM Tris-HCl, 1 mM EDTA, 0.5% NP-40, 0.5% sodium deoxycholate, pH 8, supplemented with 1:1000 dilution of protease inhibitor), and finally TE buffer (1 time, protease inhibitor-free (Corning)). Immunoprecipitated chromatin was freed from histones and Dynabeads by incubating the samples for 1 hour, 37°C with proteinase K (Qiagen) at a final concentration of 0.50 mg/mL. Chromatin samples were then purified by the Qiagen QIAquick PCR Purification Kit (Qiagen) and eluted with 50 µL of the EB buffer provided in the kit. Libraries were prepared at the Epigenomics Core using the TruSeq ChIP Library Preparation Kit (Illumina). Input and IP DNA (5-10 ng) was blunt-ended and phosphorylated, followed by the addition of a single adenine nucleotide, prior to ligation with an adaptor duplex with a T overhang. Ligated products were size-selected by agarose gel electrophoresis, purified, and PCR-amplified for the final library preparation. Quality control was performed on each input/IP library generated using loci specific primers to verify that the original enrichment was retained in the final library. Input/IP libraries that pass this quality control were then sequenced on an Illumina NovaSeq 6000 platform.

For ChIP-Seq data analysis, the ChIP-seq raw data quality was assessed using FastQC 0.11.3, and the adaptors were trimmed using TrimGalore 0.4.4. ChIP-seq and input reads were aligned to the mouse reference genome (mm10) using bowtie2[83] with default options, and the

unique map reads were extracted for peak calling. The post-alignment quality control envisulaized were performed by Deeptools 2 3.5.1.[84] PePr[85] was used to identify the differential peaks between WT-IDH1 and mIDH1 groups using FDR < 0.05 and fold-change > 3 as the cutoffs. The identified peaks were annotated to genomic features 1-5 kb upstream of promoter, promoter, intron, exon, UTR, CDS, and intergenic (using Bioconductor *annotatr* package.[86] As a comparison, the same number of peaks were randomly generated across the same chromosome and annotated the same way by *annotatr*. Gene set enrichment testing was performed on the identified differential peaks by Bioconductor package *ChIPenrich*[87] to detect enriched Gene Ontology Biological Process Terms.

Cleavage Under Targets & Release Using Nuclease (CUT&RUN)

CUT&RUN was performed using CUTANA ChIC/CUT&RUN kit (Epicypher #14-1048) following manufacturer's protocol. Briefly, 1×10^6 NS cells were coupled with Concanavalin A beads, permeabilized with 0.01% Digitonin and incubated overnight at 4°C with 0.5 µg target antibody in antibody buffer (H3K4me3 Antibody - SNAP-Certified™ for CUT&RUN, Epicypher #13-0041, H3K27ac Antibody, SNAP-Certified™ for CUT&RUN and CUT&Tag, Epicypher #13-0059). The following day, cells were first incubated for 10 min with micrococcal nuclease fused to proteins A and G (pAG-MNase), which was then activated by $CaCl_2$ addition. After 2 hours incubation at 4°C, the reaction was stopped with stop buffer and E. coli DNA was added as spike-in DNA. DNA was then isolated using SPRI beads and quantified with Qubit. Libraries were prepared using CUTANA™ CUT&RUN Library Prep Kit, following manufacturer's recommendations. Fragment size was detected using a Tape Station system and multiplexed libraries were sequenced on AVITI24 sequencer (Element Biosciences) at 150bp paired end reads. Data analysis was performed the same way as described in ChIP-Sequencing section.

Human Single Cell RNA-seq

Human glioma scRNA-seq was performed and analyzed as previously described.[12] The data has been deposited in NCBI's Gene Expression Omnibus with identifier GSE. Briefly, primary mIDH1 human glioma cells, SF10602, cultured for 7 days, in presence or absence of specific $IDH1^{R132H}$ inhibitor AGI-5198. 3' single cell libraries were generated using the 10X Genomics Chromium Controller following the manufacturer's protocol for 3' V3.1 chemistry with NextGEM Chip G reagents (10X Genomics). Final library quality was assessed using the Tapestation 4200 (Agilent), and libraries were quantified by Kapa qPCR (Roche). Pooled libraries were subjected to 150 bp paired-end sequencing according to the manufacturer's protocol (Illumina NovaSeq 6000). Raw sequencing data files were converted to fastq files and aligned to the human reference genome hg38 using the Cell Ranger Pipeline 7.0.0 (10X Genomics). The data were clustered, and gene expression were analyzed using the Seurat R package. Pathway enrichments were performed by Gene Set Variation Analysis (GSVA) package.[88]

For human samples, freshly isolated primary tumor tissue was kept in DMEM/F12 media (Gibco) as described previously.[12] Briefly, tissue was cut into small pieces until a homogenous solution is obtained. Cells were dissociated using StemPro Accutase® cell dissociation reagent (Gibco) in two-cycles of 5 min each until single-cell suspension was obtained. The cell suspension was passed through 70 μm strainer to remove debris and connective tissue, lysed with RBC's lysis buffer (Biolegend), and passed through dead cells removal column (Miltenyi Biotec). A yield of at least > 90% live cells was considered adequate for single-cell RNA-sequencing. Single cell suspensions were subjected to final cell counting on the Countess II Automated Cell Counter (ThermoFisher) and diluted to a concentration of 700 -1000 cells/ul. 3' single cell libraries were generated using the 10X Genomics Chromium Controller and following the manufacturer's protocol for 3' V3.1 chemistry with NextGEM

Chip G reagents (10X Genomics). Final library quality was assessed using the Tapestation 4200 (Agilent), and libraries were quantified by Kapa qPCR (Roche). Pooled libraries were subjected to 150 bp paired-end sequencing according to the manufacturer's protocol (Illumina NovaSeq 6000). Bcl2fastq2 Conversion Software (Illumina) was used to generate de-multiplexed Fastq files and CellRanger Pipeline (10X Genomics) was used to align reads and generate count matrices. Two biological replicates for each condition (*wtIDH1* and *mIDH1*) were analyzed. An average sequencing depth of 20,000 reads/cell was recovered for each sample we processed.

Human glioma cells stably transfected to express IDH1^{R132H}

SJGBM2 pediatric glioma cells are ATRX mutant, and they were cultured in IMDM medium with L-glutamine (0.3 mg/mL) (Gibco, 12440061), 20% FBS (Peak Serum, PS-FB3), and antibiotic-antimycotic (1X) (Gibco, 15240-062) at 37°C, 5% CO_2. SJGBM2 cells were seeded in a 6-well plate (1.5 x 10^5 each per well), and after 24h they were transfected with p-CMV-IDH1^{R132H}-Entry plasmid using jetPRIME transfection system (VWR, 89129-922). One day after transfection, the medium was replaced by selection medium containing G418 (Gibco, 10131027) at a concentration of 800 µg/mL. On day 15 of selection, individual cell colonies were taken from the well using autoclaved filter paper squares (2x2 mm approx.) previously embedded in HyQTase Cell Detachment Solution (TroyBiologicals, SV3003001) and placed within wells of 24-well plates with the appropriate cell culture medium. After 24h, the medium was replaced with selection medium. Each well corresponded to an isolated colony that was expanded for in vitro experiments. IDH1^{R132H} protein expression was confirmed by WB assay [15]. For reduced growth conditions, FBS was reduced to a final concentration of 5%.

Metabolomics profiling

Mutant IDH1 and WT NS (3 X 10^6 cells) were seeded in a T75 flask in complete media as described previously. A parallel plate for protein estimation and sample normalization was

also set up with the same number of cells. After overnight incubation, the culture media was aspirated off and replaced with fresh media. The cells were then cultured for a further 24h. For intracellular metabolites, the media was aspirated off and the samples washed once with 1 mL cold PBS before incubation with 1 mL ice cold 80% methanol on dry ice for 10min. Thereafter, cell lysates were collected from each well and transferred into separate 1.5 mL Eppendorf tubes. The samples were then centrifuged at 12,000xG, and the vol of supernatant to collect for each experimental condition was then determined based on the protein concentration of the parallel plate. The collected supernatants were dried using SpeedVac Concentrator, reconstituted with 50% v/v methanol in water, and analyzed by mass spectrometry and processed as previously described.[89] Heatmaps were plotted with Heatmap2 package in R.

Generation of human glioma NS from patient tumor biopsies

SF10602 cells were generated in Dr. Joseph Costello's laboratory at UCSF from resected biopsies from patients harboring mIDH1 tumors with TP53 and ATRX mutation.[45] SF10602 were cultured and maintained in serum free glioma neural stem (GNS) cell medium comprises of Neurocult NS-A (StemCell Technologies, 05750) supplemented with 2 mM L-glutamine (Gibco, 25030081), N-2 (Gibco, 17502-048), B-27 (without vitamin A, Gibco, 12587-010), Normocin (100 μg/ml) (InvivoGen, ant-nr-1), 0.1 mg/mL sodium pyruvate (Gibco, 11360-070) and Antibiotic-Antimycotic (1X) (Gibco, 15240-062) at 37°C, 5% CO_2. Human EGF (animal-free; PeproTech, AF-100-15), human FGF (animal-free; PeproTech, 100-18B) and PDGF-α (animal-free; PeproTech, 100-13A) were added twice weekly using 1μL of 20 ng/μL stock solution for each growth factor, equivalent to 1000X formulation per 1mL medium. For reduced growth conditions, human-EGF, human-FGF, and PDGF-α were added twice weekly at 1 μL (20 ng/μL) per 3 mL medium for a final concentration of 6.6 ng/mL.

Western blot

Mouse NS and human glioma cells (1.0 x 10^6 cells) were harvested for each genotype, and total protein extracts were prepared in a RIPA lysis and extraction buffer (Thermo Fisher Scientific, Pierce, 89900) with 1X of Halt protease and phosphatase inhibitor cocktail (Thermo Fisher Scientific, 78442). 20 μg of protein extract (determined by bicinchoninic acid assay (BCA), Pierce, 23227) were separated by 4-12% SDS-PAGE (Thermo Fisher Scientific, NuPAGE, NP0322BOX) and transferred to nitrocellulose membranes (Bio-Rad, 1620112). The membrane was probed with 1:2000 of a rabbit anti-ATG9b Ab (Novus Biologicals, NBP1-77169), 1:1000 of a rabbit anti-ATG7 Ab (Cell Signaling Technology, 8558S), 1:1000 of a rabbit anti-pULK1 (S555) Ab (Cell Signaling Technology, 5869); 1:1000 of a rabbit anti-pULK1 (S757) Ab (Cell Signaling Technology, 6888); 1:1000 of a rabbit anti-ULK1 (Cell Signaling Technology, 8054); 1:2000 of a rabbit anti-MST4 Ab (Abcam, ab52491); 1:1000 of a rabbit anti-ATG4b Ab (Cell Signaling Technology, 5299); 1:1000 of a rabbit anti-phosphoATG4b Ab (Cell Signaling Technology, 19386); 1:1000 of an anti-UVRAG Ab (Abcepta, AP1850d); 1:1500 of a rabbit anti-LC3 I/II Ab (Novus Biologicals NB100-2220); 1:2000 of an anti-β-actin Ab (Cell Signaling Technology, 3700), then followed by secondary [Dako, Agilent Technologies, goat anti-rabbit 1:4000 (P0448), rabbit anti-mouse 1:4000 (P0260)]. Enhanced chemiluminescence reagents were used to detect the signals following the manufacturer's instructions (SuperSignal West Femto, Thermo Fisher Scientific, 34095). Blots were imaged using a ChemiDoc (Bio-Rad ChemiDoc™ MP System). WB quantification was performed using ImageJ, and the reported data are from three replicates. For the cells treated with α-ketoglutarate (α-KG), mIDH1 mouse NS (5.0 x 10^5 cells) were treated with 2.5 mM α-KG (Cayman Chemicals, 876150-14-0) for 5 hours prior to protein extraction.

Western Blot Assay of Histones

To assess specific histone markers post translational modifications, histone extracts were obtained using Histone Purification Mini Kit (Active Motif, 40026) and WB were

performed on 1.5 μg of histone extract. Histone markers' specific antibodies were as follows: 1:1000 of H3K4me3 antibody (Hologic Diagenode, C15410003); 1:1000 of H3K36me3 antibody (Hologic Diagenode, C15410192); 1:2000 of H3K27me3 antibody (Millipore, B07-449) for human glioma cell protein extracts; 1:1000 of H3K27me3 antibody (Hologic Diagenode C1541095); and 1:2000 of total histone H3 antibody (Cell Signaling Technologies, 4499).

Metabolic Flux Assay

To assess metabolic activity, oxygen consumption rates (OCR) and extracellular acidification rates (ECAR) were performed using the XF-96 Extracellular Flux Analyzer (Agilent). Cells were washed and resuspended in nonbuffered DMEM, adjusted to pH~7.4. WT-IDH1 and mIDH1 cells ($1x10^5$ cells/well) were seeded on laminin-coated plates and allowed to equilibrate for 30min in a non-CO_2, 37ºC incubator. OCR and ECAR were measured under basal conditions and in response to the following mitochondrial inhibitors: oligomycin (1 μM), FCCP (1 μM), rotenone (100 nM), and antimycin A (1 μM). After the assay, OCR and ECAR measurements were normalized to cell number using CyQuant NF analysis (Invitrogen). For R-2HG treatment, cells were incubated in 2.5 mM of (2R)-Octyl-α-hydroxyglutarate for 5h before assessing metabolic activity.

Mitochondria staining

To assess the mitochondrial morphology, cells (1×10^5 cells) were plated and were left overnight in 37°C incubator with 5% CO_2. Following incubation, cells were labeled with MitoTracker Green FM (50 nM, Thermo Fisher Scientific, M7514) for 45 mins according to the manufacturer's instructions with slight modification. Cells were also stained with Hoechst 33342 dye (5 μM; Invitrogen Fisher Scientific, H3570) for 20 mins to label the nucleus. Cells were subsequently rinsed with HBSS and replaced by fresh growth medium before analyzed through confocal microscopy.

Autophagy flux assay using mCherry-GFP-LC3 construct

Lentiviral particles expressing mCherry-GFP-LC3 were generated by the University of Michigan Vector Core using the FUW mCherry-GFP-LC3 plasmid,[56] which was gift from Anne Brunet. WT-IDH1 and mIDH1 SJGBM cells were cultured in a T-12.5 flask and infected with Lenti-mCherry-GFP-LC3 particles in a concentration of 1X of lentivirus. After 36h, $5x10^4$ cells were plated in a confocal microscopy chamber cover glass system, in presence or absence of 10 μM of chloroquine and cultured for 12h before analysis of GFP and mCherry expression by confocal microcopy.

Confocal microscopy and image analysis

Cells were placed into the incubator chamber of the microscope at 37°C with a 5% CO_2 atmosphere. Microscopy confocal images were acquired using a single photon laser scanning inverted confocal microscope LSM 880 AxioObserver (Carl Zeiss, Jena, Germany). Two laser lines were used for simultaneous excitation with a Plan-apochromat 63x/1.4 numerical aperture (NA) oil DIC M27 objective. Cells transfected with mCherry-GFP-LC3 were excited at 488 nm and 561 nm, and cells stained with MitoTracker™ green dye at 405 nm and 488 nm wavelength, respectively. Line-sequential scan mode and 1.4 scan zoom were used. The system was driven by ZEN Black software. Multichannel immunofluorescence images were processed and analyzed using Fiji (NIH). Autophagosome (green) and autolysosome (red) were manually identified and quantified using the plugging Cell Counter.

In vitro experiments with radiation and autophagy inhibitors

WT-IDH1 and mIDH1 mouse NS and human glioma cells (i.e., NPA/NPAI, SJ-GBM2/SJ-GBM2 mIDH1, and SF10602/SF10602 with AGI-5198) were plated at a density of $1x10^3$ cells/well in a 96-well plate 24h before treatment. WT-IDH1 and mIDH1 mouse NS (NPA/NPAI) were then incubated with either ATG7 siRNAs (100 nM; Origene, SR427399), ATG4b siRNAs (100 nM; Origene, SR413163), ULK101 (1 μM; SelleckChem, S8793), or

NSC185058 (5 μM; Cayman Chemical, 23957) in combination with 3Gy of IR, 2h post-inhibitor treatment. Human glioma cells (SJGBM2/SJGBM2 mIDH1, and SF10602/SF10602 with AGI-5198) were then incubated with either ATG7 siRNAs (150 nM; Origene, SR323157), ATG4b siRNAs (150 nM; Origene, SR323518), ULK101 (3 μM; SelleckChem, S8793), or NSC185058 (15 μM; Cayman Chemical, 23957) in combination with 5Gy (SJGBM2/SJGBM2 mIDH1) or 20Gy (SF10602/SF10602 with AGI-5198) of IR, 2h post-inhibitor treatment. Cell viability was evaluated 72h post-IR treatment using CellTiter-Glo 2.0 (Promega, G9242) luminescence cell viability assay, following the manufacturer's protocol. The resulting luminescence was read with the Enspire Multimodal Plate Reader (PerkinElmer, 2300-0000). Data were represented graphically using GraphPad Prism software (version 8), and statistical significances were determined using one-way ANOVA followed by Tukey's test for multiple comparisons.

In vitro Dose-Response and evaluation of radio-sensitivity using mitochondrial electron transport chain inhibitors

To assess the susceptibility of both mutant and WT-IDH1 human (SJ-GBM2 WT-IDH1/ SJ-GBM2 mIDH1 and SF10602/SF10602 with AG-881) and mouse NS (NPA/NPAI, CPA/CPAI, and RPA/RPAI) to mitochondrial electron transport chain inhibitors (mETCi), two Complex I inhibitors were used: Rotenone (SelleckChem, S2348) and Metformin (SelleckChem, S1950) under normal and growth factor starved conditions. Both cell lines were plated at a density of 1000 cells per well in a 96-well plate (Fisher, 12-566-00) 24h prior to treatment where wells per inhibitor dose (1 μM, 2.5 μM, 5 μM, 10 μM, 20 μM, and 30 μM) were evaluated for each cell type. Cells were then incubated for 3 days under normal (EGF: 1:1000, FGF: 1:1000, and PDGFα: 1:1000 dilutions) as well as growth factor starved conditions (EGF: 1:3000, FGF: 1:3000, and PDGFα: 1:3000 dilutions) and viability was assessed using CellTiter Glo 2.0 assay (Promega, G9242) following manufacturer's protocol. To assess radio-sensitivity of each cell

line, cells were incubated with either free-Rotenone or Metformin, or in combination with radiation at their respective IC50 doses for 72 hours in triplicate wells per condition. Cells were pre-treated with both the inhibitors 2 hours prior to IR with 3Gy for mouse, 5Gy for SJ-GBM2 and 20Gy for SF10602 of radiation, respectively. Resulting luminescence was read with the Enspire Multimodal Plate Reader (PerkinElmer, 2300-13 0000).

Release of cytokines in response to autophagy inhibition and radiation

To assess the release of cytokines (DAMPs and type-I IFNs) into the conditioned media, mIDH1 mouse NS and human glioma cells were seeded at a density of $1x10^6$ cells/well in 6-well plates and allowed to settle overnight before treatment. The following day, mIDH1 mouse NS were treated with either ATG7 (100nM; Origene, SR427399) or ATG4b (100nM; Origene, SR413163) for 2h prior to exposure to 3Gy of IR, and the human glioma cells were treated with either ATG7 (150nM; Origene, SR323157) or ATG4b (150nM; Origene, SR323518) for 2h prior to exposure to 5Gy of ionizing radiation. After 72h, the levels of various cytokines in the cultures' supernatants were measured using ELISA, either following the manufacturer's protocol (Novus Biologicals) or at the Cancer Center Immunology Core, University of Michigan.

Implantable syngeneic murine glioma models

Female C57BL/6 mice, aged 6-8wk old, were used for implantation models. Intracranial tumors were established by stereotactic injection of $5x10^4$ WT-IDH1 or mIDH1 mouse tumor NS into the right striatum using a 22-gauge Hamilton syringe (1 μL/min) with the following coordinates: +1.00 mm anterior, 1.8 mm lateral, and 3.5 mm deep. The presence of tumors was verified 5 days post-implantation (DPI) by bioluminescence imaging.

Generation of autophagy deficient glioma cells using SB transposon system

Our laboratory has modelled both high grade glioma and mIDH1 low grade glioma by integrating oncogenic plasmid DNA into the neural stem cells present within the developing

brain of post-natal mice utilizing the sleeping beauty (SB) transposon system. The high-grade glioma cells endogenously express genetic lesion that drive oncogenesis through NRASG12V and simulate tumor suppressor loss by ATRX and TP53 short hairpin knockdown; thus named NPA (NRASG12V, TP53, and ATRX) hereafter. The mIDH1 glioma cells endogenous express $IDH1^{R132H}$ along with genetic lesions that drive oncogenesis through NRASG12V and simulate tumor suppressor loss by ATRX and TP53 short hairpin knockdown; thus named NPAI (NRASG12V, TP53, ATRX, and $IDH1^{R132H}$) hereafter. Tumor NS were derived from endogenous NPA tumors that were adapted to in vitro culture and could be reimplanted into immunocompetent C57BL6 (The Jackson Laboratory, C57BL/6J Strain# 000664) mice for preclinical experiments in this study.

Sleeping-beauty derived glioma cells NPA and NPAI were transfected using jetPEI (VWR, catalog 89129-960) with the plasmid pT2-shATG7-EBFP and sleeping beauty transposase plasmid (Supplementary Fig. 30a-b). After transfection, cells were allowed to grow for 72h then they were subjected to FACS for isolation of BFP cells. These cells were sorted 3 times each before confirming ATG7 knockdown via Western Blot assay (Supplementary Fig. 30c-d).

Generation of autophagy deficient mouse model using SB transposon system

Using the SB transposon system,[78] we generated a glioma model harboring $IDH1^{R132H}$, shATRX, and shP53 as previously described,[15] plus a shRNA for ATG7 (shATG7) to disrupt the autophagy pathway into the tumor. The shATG7 candidates were obtained from codex database (http://cancan.cshl.edu/cgi-bin/Codex/Codex.cgi) and cloned into the pT2 plasmid replacing shATRX sequences from our previous PT2-shATRX construction,[79] generating the pT2-ATG7-BFP (Supplementary Fig. 30). A WB assay was performed to select the best candidate to use for the generation of the animal model. The selected shATG7-A (HP_603911) (CTCGAGTGCTGTTGACAGTGAGCGACCAGAAGAAGTTGAACGAGTATAGTGAA

GCCACAGATGTATACTCGTTCAACTTCTTCTGGGTGCCTACTGCCTCGGAGAATT C) was finally used in the combination cocktail of plasmids as described in Supplementary Fig. 30a-b.

Genetically engineered mutant IDH1 glioma model

All animal studies were conducted according to guidelines approved by the IACUC at the University of Michigan. All animals were housed in an AAALAC accredited animal facility; and they were monitored daily. Studies did not discriminate sex, and both male and females were used. The strains of mice used in the study were C57BL/6 (The Jackson Laboratories, 000664).

The wild type (WT)-IDH1 and mIDH1 glioma models used in this study were generated previously for our group using SB Transposon System.[15] The plasmid used to generate those models are: (i) SB transposase and LUC (pT2C-LucPGK-SB100X, henceforth referred to as SB/Luc), (ii) a constitutively active mutant of NRAS, NRAS-G12V (pT2CAG-NRASV12, henceforth referred to as NRAS), (iii) a short hairpin against p53 (pT2-shp53-GFP4, henceforth referred to as shp53), (iv) a short hairpin against ATRX (pT2-shATRX53-GFP4, henceforth referred to as shATRX), and (v) mutant $IDH1^{R132H}$ (pKT-$IDH1^{R132H}$-IRES-Katushka, henceforth referred to as mIDH1). Neonatal P01 C57BL/6 mice were used in all experiments. The genotype of SB- generated mice involved these combinations: (i) NRAS, shP53, and shATRX (WT-IDH1) and (ii) NRAS, shp53, shATRX, and $IDH1^{R132H}$ (mIDH1). Mice were injected according to a previously described protocol.[78] Plasmids were mixed in mass ratios of 1:2:2:2 or 1:2:2:2:2 (20 μg plasmid in a total of 40 μL plasmid mixture) with in vivo-jetPEI (Polyplus Transfection, 201-50G) (2.8 μL per 40 μL plasmid mixture) and dextrose (5% total) and maintained at room temperature for at least 15 min prior to injection. The lateral ventricle (1.5 mm AP, 0.7 mm lateral, and 1.5 mm deep from lambda) of neonatal mice (P01) was injected with 0.75 μL plasmid mixture (0.5 μL/min) that included: (1) SB/Luc, (2) NRAS, (3)

shp53, (4) with or without shATRX, and (5) with or without IDH1^{R132H}. To monitor plasmid uptake in neonatal pups, 30 μL of luciferin (30 mg/mL) was injected s.c. into each pup 24-48h after plasmid injection. In vivo bioluminescence was measured on an IVIS Spectrum (Perkin Elmer, 124262) imaging system. For the IVIS spectrum, the following settings were used: automatic exposure, large binning, and aperture f=1. For in vivo imaging of tumor formation and progression in adult mice, 100 μL of luciferin solution was injected i.p. and mice were then anesthetized with oxygen/isoflurane (1.5-2.5% isoflurane). To score luminescence, Living Image Software Version 4.3.1 (Caliper Life Sciences) was used. A region of interest (ROI) was defined as a circle over the head, and luminescence intensity was measured using the calibrated unit's photons/s/cm2/sr. Multiple images were taken over a 25min period following injection, and maximal intensity was reported.

For survival studies, animals were monitored daily for signs of morbidity, including ataxia, impaired mobility, hunched posture, seizures, and scruffy fur. Animals displaying symptoms of morbidity were intracardially perfused using Tyrode's solution, followed by fixation with 4% paraformaldehyde (PFA) in PBS.

Generation of iRGD Synthetic Protein Nanoparticle (SPNP) with siRNA against *ATG7*

SPNP formulation:

The preparation of the SPNP formulations followed previously reported methods but with modifications [44]. In the basic formulation, two solutions were prepared separately then combined. HSA (7.5% w/v) was solubilized in a solvent system comprised of ultrapure deionized water and ethylene glycol (80:20 v/v). The peptide, iRGD was then added along with BSA Alexa Fluor 647 conjugate (0.25% w/w relative to the albumin) to produce fluorescently labeled SPNPs. Then, the siRNA, which was resuspended according to the manufacturer's protocol, was complexed for 30min at room temperature under rotation with 60 kDa branched polyethyleneimine (5% w/v) before also being added to the serum albumin solution. Next, a

bi-functional macromer, O,O'-Bis[2-N-Succinimidyl-succinylamino)ethyl]polyethylene glycol, was added at 10% w/w relative to the HSA solution. Once mixed, the two solutions were mixed to form the final formulation. For empty SPNP groups, all the components that were added in the iRGD ATG7i-SPNPs were included except for the ATG7 siRNA.

SPNP fabrication

SPNPs were fabricated via electrohydrodynamic jetting.[44] The parameters used were the same as previously described. Briefly, the final formulation was loaded into 1 mL syringes equipped with a 1.5" 25-gauge stainless steel blunt needle. It was pumped at a rate of 0.2 mL/h to form droplets at the base of the needle. A voltage source was connected to the needle and grounded at the collection plate, located 6 inches from the base of the pump. The voltage was adjusted typically to a range between 8 kV and 15 kV to achieve a stable Taylor cone whereby rapid evaporation of the solvent occurred, creating solid nanoparticles on the collection plate. The collection plate was replaced with a clean plate every 30min until the solution within the syringe emptied. The collection plates were enclosed and incubated for 7 days at 37°C to form stable crosslinks.

SPNP collection and processing

After the 1wk period of incubation, the SPNPs on collection plates were removed. About 3-4mL of 0.01% Tween 20 in DPBS was added to each pan and physically agitated with plastic razor blades to release the SPNPs off the plate. The SPNP suspension was collected into a falcon tube. Each pan was agitated with fresh 0.01% Tween 20 in DPBS three times. The collected SPNPs was tip sonicated at an amplitude of 7 for 30s (1s on and 3s off) in an ice bath to break up aggregates, strained through a 40 μm filter into a new falcon tube then centrifuged at 3220 RCF for 5min. The supernatant was removed and distributed into 2 mL Eppendorf tubes and centrifuged for 1h at 4˚C at 21,500 RCF. The supernatant was discarded, and the

resulting pellets were combined into a single 2 mL tube. The particles were washed two times with fresh DPBS without Tween 20.

SPNP characterization

Scanning electron Microscopy: Scanning electron microscopy samples were prepared by placing a silicon wafer on top of the collection plate during the jetting process. The samples were then placed on a copper tape covered scanning electron microscopy stub, then gold coated for 40s and visualized through the FEI NOVA 200 SEM/FIB instrument. The dry state SPNP quantification of morphology parameters were conducted through ImageJ analysis as described previously.[90]

Dynamic Light Scattering: The hydrodynamic diameter and zeta potential was determined through dynamic light scattering on the Malvern Zetasizer. Samples were prepared by diluting the stock sample in DPBS and measured in folded capillary zeta cells. An average of at least three measurements was used to characterize each sample.

Bicinchoninic acid assay (BCA assay): BCA assay was used to quantify SPNP concentration. A standard curve was prepared for every SPNP concentration quantification measurement.

In vitro mouse T cell proliferation assay

To evaluate the effect of the combination of radiation (IR) treatment and autophagy inhibition, we tested the effect of IR (2 Gy) and the administration of iRGD nanoparticles loaded with a siRNA against *ATG7* (ATG7i-SPNP) in vivo. Twenty mice were implanted with mIDH1-OVA mouse tumor NS as stated above, and 7 days post implantation, mice were divided in the following 4 groups (n=5 mice): Control (no treatment); ATG7i-SPNP only; IR only; and IR + ATG7i-SPNP. Mice were treated with 2 Gy IR, for five consecutive days. ATG7i-SPNP ($2.0x10^{11}$ particles) were administered 3 times total, once every other day

starting on day 5. The mice were euthanized, and the spleens were collected on day 21 post implantation.

The spleens were collected to analyze the development of anti-tumor immune response. Splenocyte processing was performed as detailed previously.[91] The splenocytes were cultured with 100 nM of SIINFEKL for 24 hours in 10% FBS-media with 55 μM 2-ME. Cells were then stained with anti-CD45, anti-CD3 and anti-CD8 antibodies, and proliferation was assessed by CFSE dye dilution. All flow data were acquired on a FACSAria flow cytometer (BD Biosciences) and analyzed using FlowJo version 10 (Treestar).

IHC of paraffin-embedded brains

Following perfusion, mouse brains were fixed in 4% paraformaldehyde (PFA) for an additional 48h at 4°C, then transferred to 70% ethanol, and processed and embedded in paraffin at the University of Michigan Microscopy & Image Analysis Core Facility using a Leica ASP 300 paraffin tissue processor/Tissue-Tek paraffin tissue embedding station (Leica). Tissue was sectioned using a rotary microtome (Leica) set to 5 μm in the z-direction. Antigen retrieval and IHC of paraffin-embedded sections were performed using antibodies and dilutions as follows: Tissue sections were blocked with blocking solution (1x PBS with 0.2% Tween-20 with 5% Goat Serum) for 2h. Sections were incubated with the following primary antibodies: anti-CD3ε (Cell Signaling, 99940); anti-CD68 (Abcam, ab125212); anti-MBP (Millipore, MAB386); anti-GFAP (Millipore, AB5541) at 4°C overnight. Tissue sections were then labeled with Secondary Biotinylated Ab (1:1000) in PBS with 0.2% Tween-20 for 15min at RT then 4°C overnight. ABC Avidin-Biotin-COMPLEX Binding was done using VECTASTATIN ABC Reagent (Vectastain Elite ABC-HRP kit; Vector Laboratories, PK-6100). Sections were incubated for 1h with VECTASTAIN ABC Reagent in the dark and then washed with gentle agitation. Colorimetric Detection of Peroxidase was performed using Betazoid DAB Chromogen kit (BioCare BDB2004) according to the manufacturer's instructions. Afterward,

Hematoxylin Counterstain was done, and coverslips were mounted with a xylene-based mounting medium and let dry on a flat surface at room temperature until imaging. Images were obtained using brightfield/epifluorescence (Zeiss Axioplan2, Carl Zeiss MicroImaging) or laser scanning confocal microscopy (Leica DMIRE2, Leica Microsystems) and analyzed using LSM5 software (Carl Zeiss MicroImaging). Immunostaining was performed using the Discovery XT processor (Ventana Medical Systems).

To access ATG7 expression levels post treatment of ATG7i-SPNPs, we implanted mice intracranially with $2x10^4$ NPAI cells on Day 0. At day 10, mice were randomly divided into 2 groups of 3 mice each. One group was treated with saline and the other group with ATG7i-SPNPs in combination with IR. Mice received a total of 10 Gy of radiation in 5 days. Mice were administered three doses of ATG7i-SPNPs ($2x10^{11}$) at day 10, 12, and day 14. At the end of day 14, mice were perfused, and brain and liver tissues were collected for further analysis. Brain sections from these mice were stained for MBP (myelin basic protein) (Sigma, MAB386), GFAP (glial fibrillary acidic protein) (Sigma, AB5541), ATG7 (Invitrogen, PIPA535203), and cleaved Caspase-3 (Cell Signaling, 9661S).

Supplementary Figure 1: Autophagy related gene expression from TCGA.

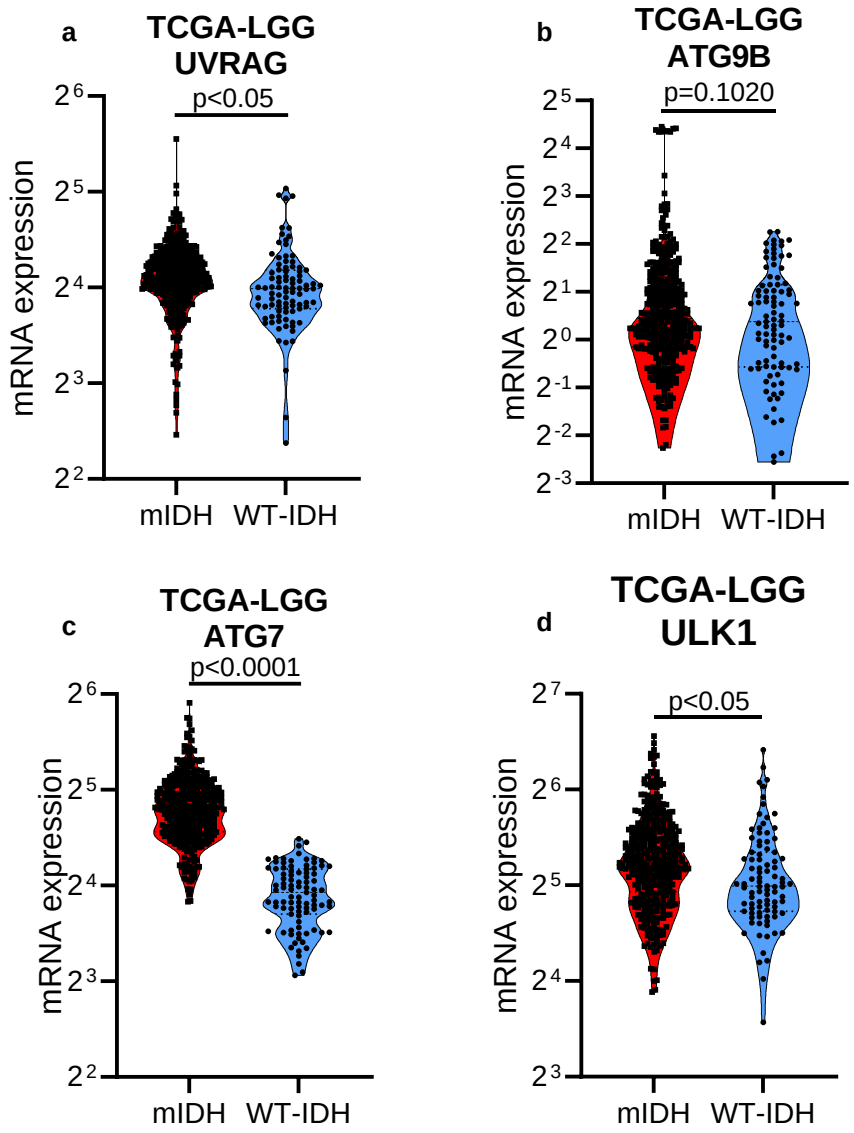

Supplementary Figure 1: Autophagy related gene expression from TCGA. (**a**) Analysis of RNA-seq data obtained from TCGA to quantify UVRAG mRNA in LGG with wtIDH1 or mIDH1. (**b**) Analysis of RNA-seq data obtained from TCGA to quantify ATG9B mRNA in LGG with wtIDH1 or mIDH1. (**c**) Analysis of RNA-seq data obtained from TCGA to quantify ATG7 mRNA in LGG with wtIDH1 or mIDH1. (**d**) Analysis of RNA-seq data obtained from TCGA to quantify ULK1 mRNA in LGG with wtIDH1 or mIDH1. Unpaired t test.

Supplementary Figure 2: Sample processing for metabolomic profiling in glioma cells.

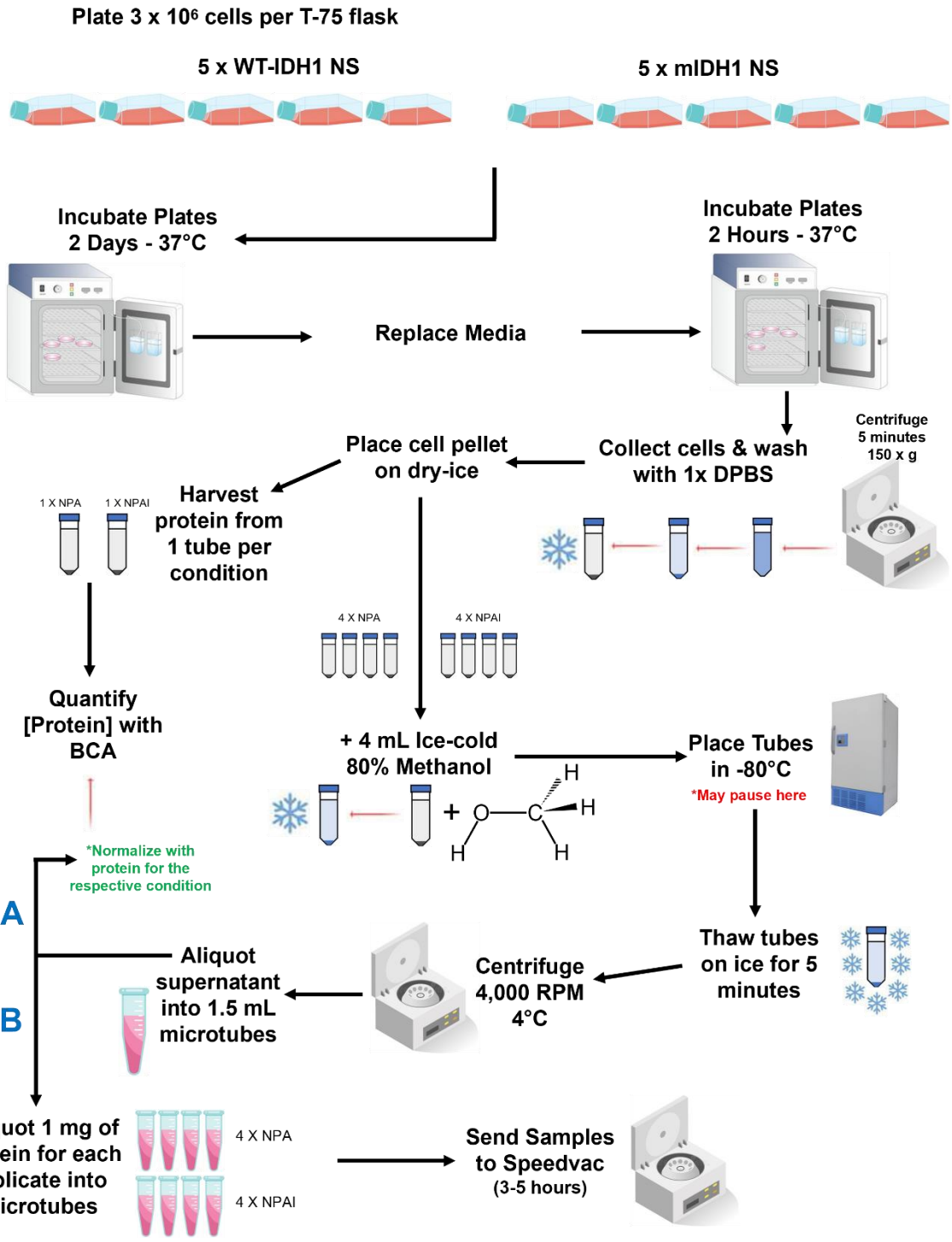

Supplementary Figure 2: Sample processing for metabolomic profiling in glioma cells.

Diagram showing the method and sample processing for metabolic profiling in glioma cells.

Supplementary Figure 3: Heatmap of the metabolites within wild-type and mutant IDH1 mouse glioma cells.

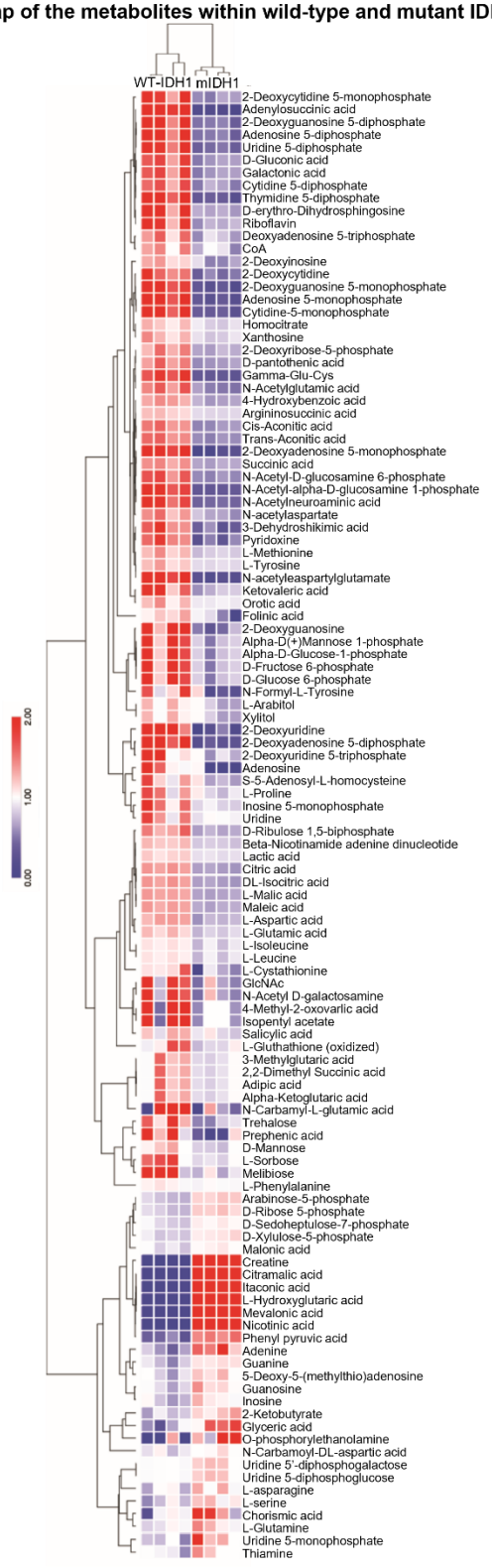

Supplementary Figure 3: Heatmap of the metabolites within wild-type and mutant IDH1 mouse glioma cells. Heatmap showing the metabolomic profiling in WT-IDH1 and mIDH1 glioma NS filtered by $P < 0.1$.

Supplementary Figure 4: Significantly different metabolites within wild-type and mutant IDH1 mouse glioma cells.

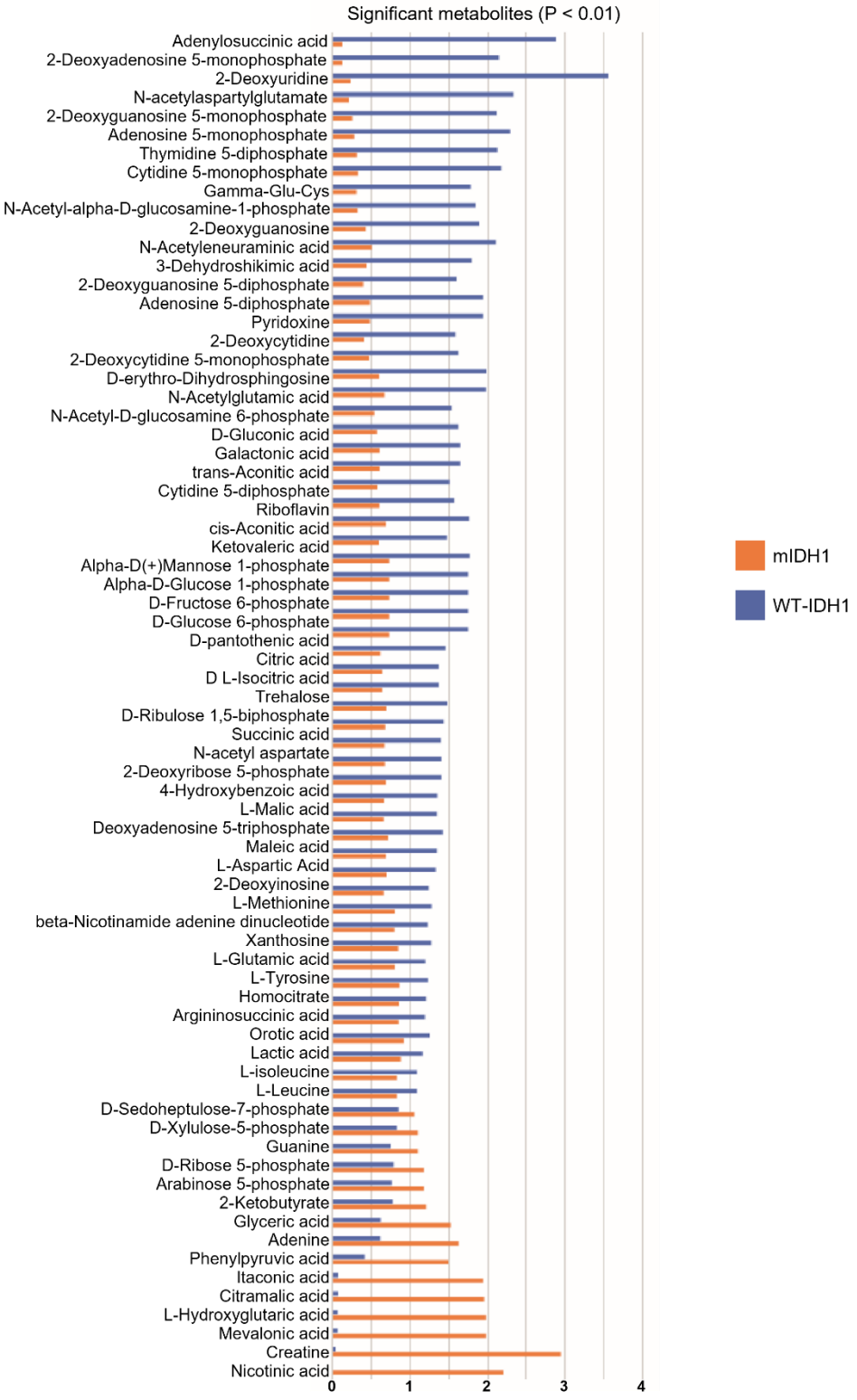

Supplementary Figure 4: Significantly different metabolites within wild-type and mutant IDH1 mouse glioma cells. Bar graph showing significantly different metabolites ($P < 0.01$) comparing the WT-IDH1 NS (blue bars) with the mIDH1 NS (orange bars) expressed in AU.

Supplementary Figure 5: Metabolic pathway analysis plat created using MetaboAnalyst.

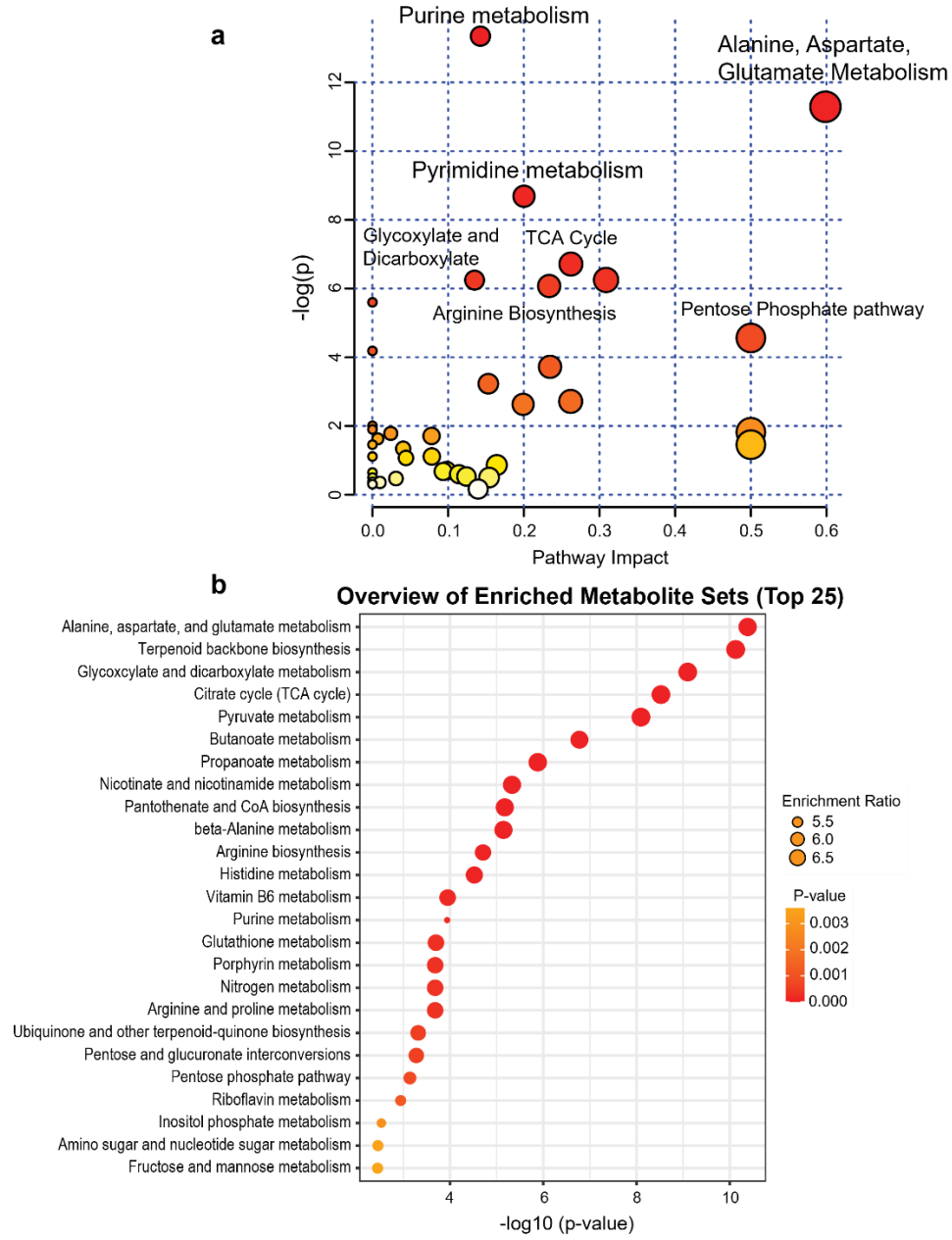

Supplementary Figure 5: Metabolic pathway analysis plot created using MetaboAnalyst. (**a**) Plots depict several metabolic pathway alterations induced in mIDH1 NS when compared with WT-IDH1 NS. The x-axis represents the pathway impact value computed from pathway topological analysis, and the y-axis is the negative log of the p-value obtained from pathway enrichment analysis. The pathways that were most significantly changed are characterized by both a high -log(p) value and high impact value (top right region). (**b**) Enrichment analysis on metabolic set alterations induced in mIDH1 NS when compared with WT-IDH1 NS.

Supplementary Figure 6: Violin plots of scRNA-seq in human mIDH1 glioma cells related to Figure 4.

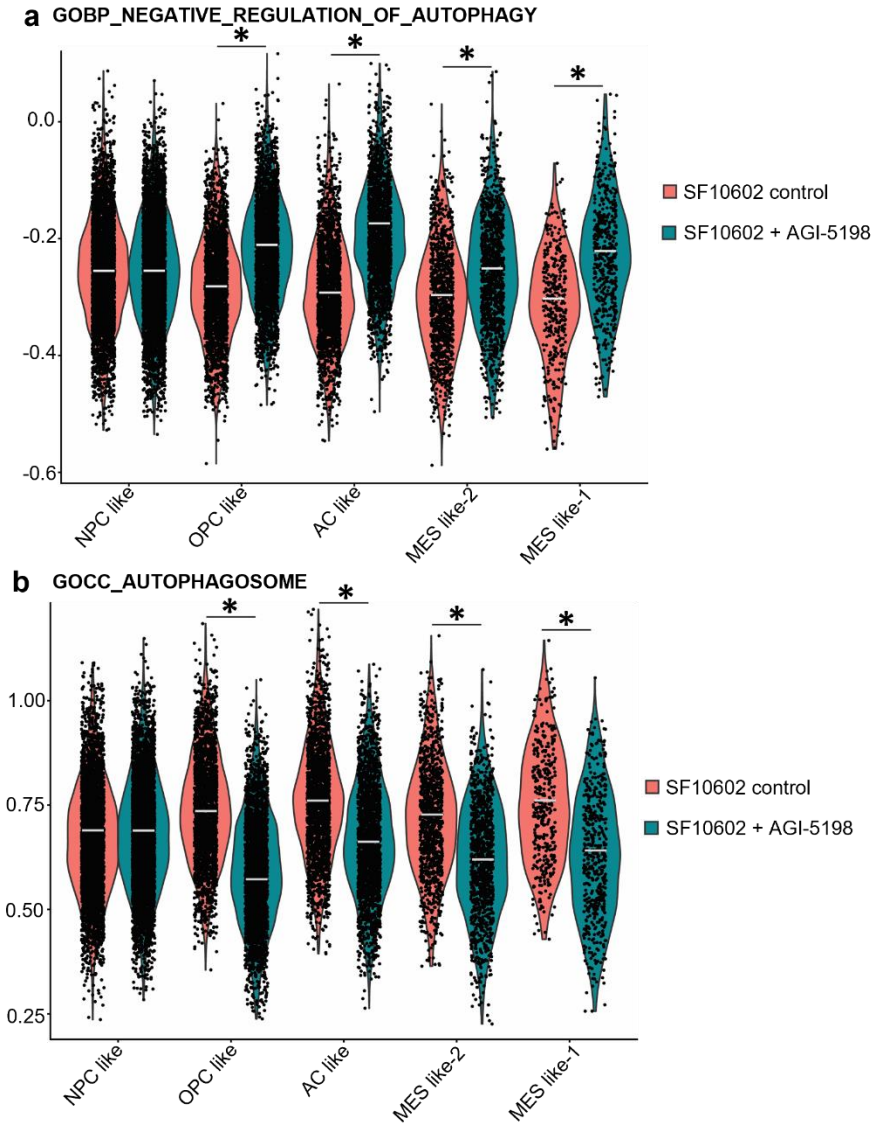

Supplementary Figure 6: Violin plots of scRNA-seq in human mIDH1 glioma cells related to Figure 4. (**a**) GO term enrichment score for GO biological process of negative regulation of autophagy. (**b**) GO term enrichment score for GO cellular component of autophagosome. Significance was measured via the Wilcoxon Rank Sum Test from the Seurat/Presto package. *$P < 0.05$.

Supplementary Figure 7: Maximal Oxygen Consumption Rate and Extracellular Acidification Rate in glioma NS.

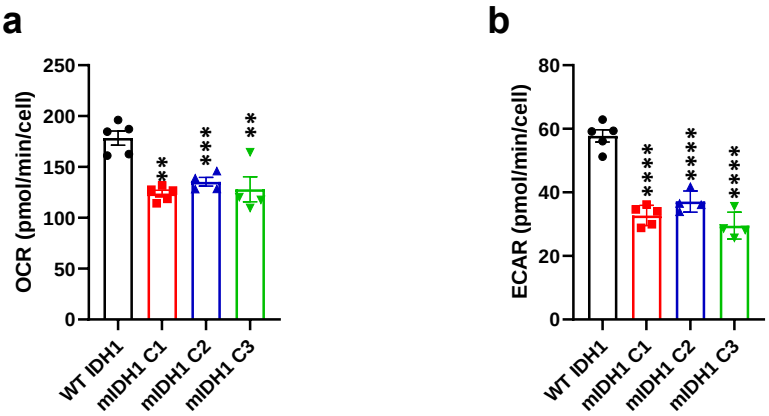

Supplementary Figure 7: Maximal Oxygen Consumption Rate (OCR) and Extracellular Acidification Rate (ECAR) in glioma NS. Mitochondrial respiration of NS derived from WT or mIDH1 tumors (Clones 1-3) examined through the Mito Stress Test. (**a**) Basal oxygen consumption rates (OCAR) and (**b**) extracellular acidification rates (ECAR) of mIDH1 and WT glioma NS. Error bars depict SD of technical replicates from a representative plot of 3 independent experiments. $^{**}P < 0.01$, $^{***}P < 0.001$, $^{****}P < 0.0001$; one-way ANOVA.

Supplementary Figure 8: Impact of mitochondrial complex 1 inhibition on glioma cell viability.

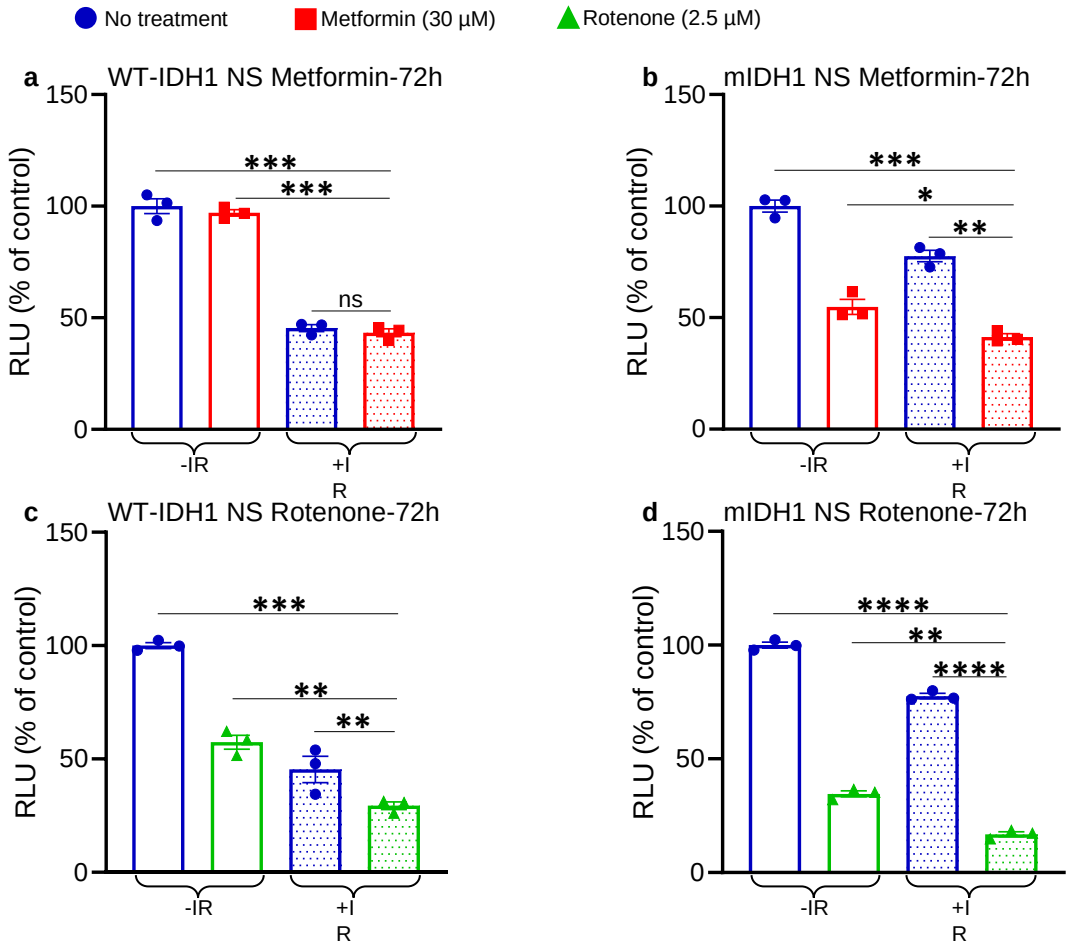

Supplementary Figure 8: **Impact of mitochondrial complex 1 inhibition on glioma cell viability.** *In vitro* inhibition of Complex I of Electron Transport Chain (**ETC**) restores radiosensitivity in mIDH1 NS. (**a-b**) Impact of Metformin on radiosensitivity in NRAS/shP53/shATRX/mIDH1 (NPAI) +/- mouse NS cells. Cell viability assay shows the effect of Metformin at 30 µM doses in combination with radiation (3 Gy) on cell proliferation in (a) WT-IDH1 and (a) mIDH1 mouse NS. Results are expressed in relative luminescence units (RLU). *P < 0.05, **P < 0.01, ***P < 0.001; two-way ANOVA followed by Tukey's test (n= 3 technical replicates). (**c-d**) Impact of Rotenone on radiosensitivity in NPAI +/- mouse NS cells. Cell viability assay shows the effect of Rotenone at 2.5 µM doses in combination with radiation (3 Gy) on cell proliferation in (c) WT-IDH1 and (d) mIDH1 mouse NS. Results

are expressed in RLU. *P < 0.05, **P < 0.01, ***P < 0.001; ****P < 0.0001; two-way ANOVA followed by Tukey's test (n = 3 technical replicates).

Supplementary Figure 9: *In vitro* inhibition of Complex I of the Electron Transport Chain induces cell death and restores radiosensitivity in two human mIDH1 glioma cells.

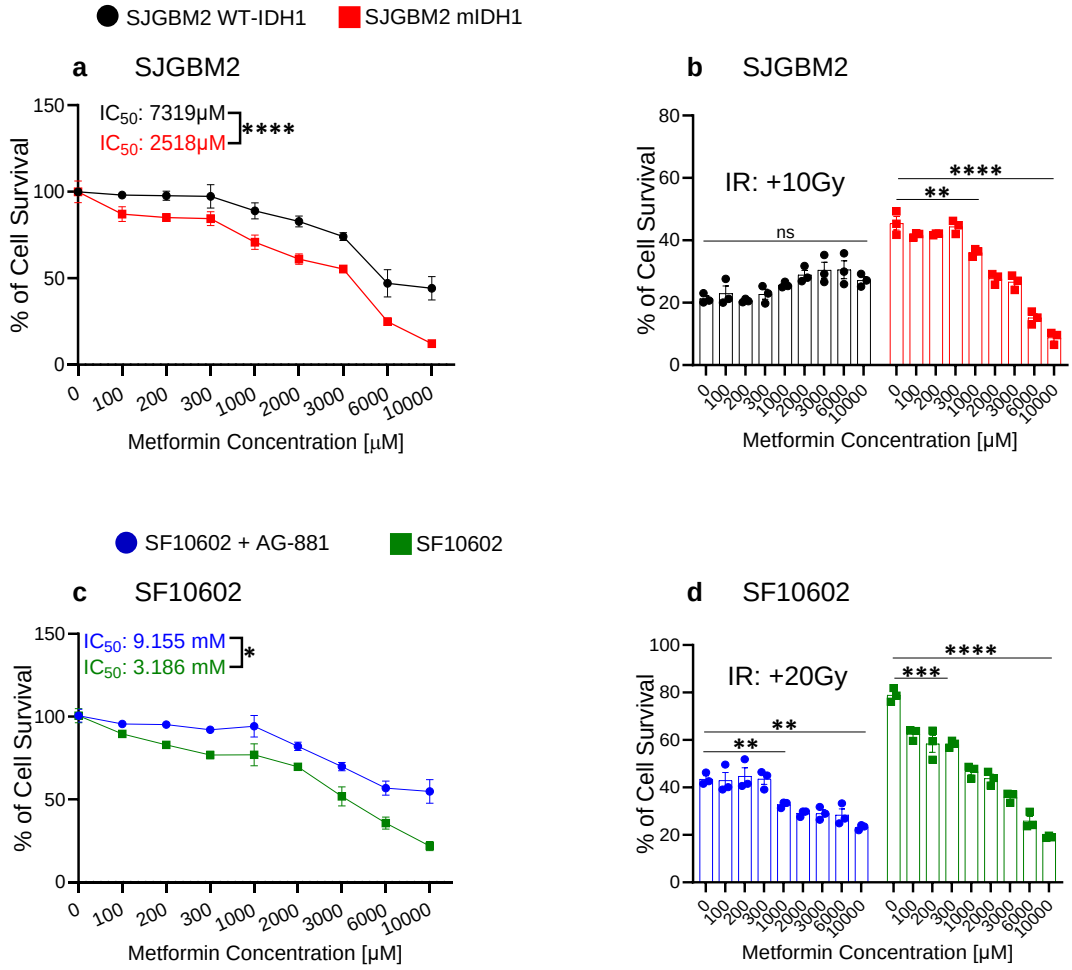

Supplementary Figure 9: *In vitro* inhibition of Complex I of the Electron Transport Chain (ETC) induces cell death and restores radiosensitivity in two human mIDH1 glioma cells. (**a**) Cell viability assay of WT-IDH1 and mIDH1 genetically engineered human glioma cells, SJGBM2, treated with metformin for 72 hours at increasing concentrations. Cell viability expressed as % of cell survival relative to control populations. A linear regression model and generalized additive models were used to determine the dose-response relationship. (**b**) Cell viability assay showing the effect of metformin at increasing concentrations in combination with radiation (10Gy) on the proliferation of WT-IDH1 and mIDH1 SJGBM2 cells. (**c**) Cell viability assay of endogenous mIDH1 glioma cells, SF10602, treated with and without mIDH1 inhibitor, AG-881, were treated with metformin for 72 hours at increasing concentrations. Cell

viability expressed as % of cell survival relative to control populations. A linear regression model and generalized additive models were used to determine the dose-response relationship. (**d**) Cell viability assay showing the effect of metformin at increasing concentrations in combination with radiation (20Gy) on the proliferation of AG-881 treated SF10602 and untreated SF10602 cells. Results are expressed as % of Cell survival relative to control populations. Statistical analyses were conducted using student's t-test and error bars depict SD of technical replicates from 3 independent experiments. *$P < 0.1$, **$P < 0.01$, ***$P < 0.001$, ****$P < 0.0001$, ns = not significant.

Supplementary Figure 10: *In vitro* inhibition of Complex I of the ETC induces cell death and restores radiosensitivity in two human mIDH1 glioma cells.

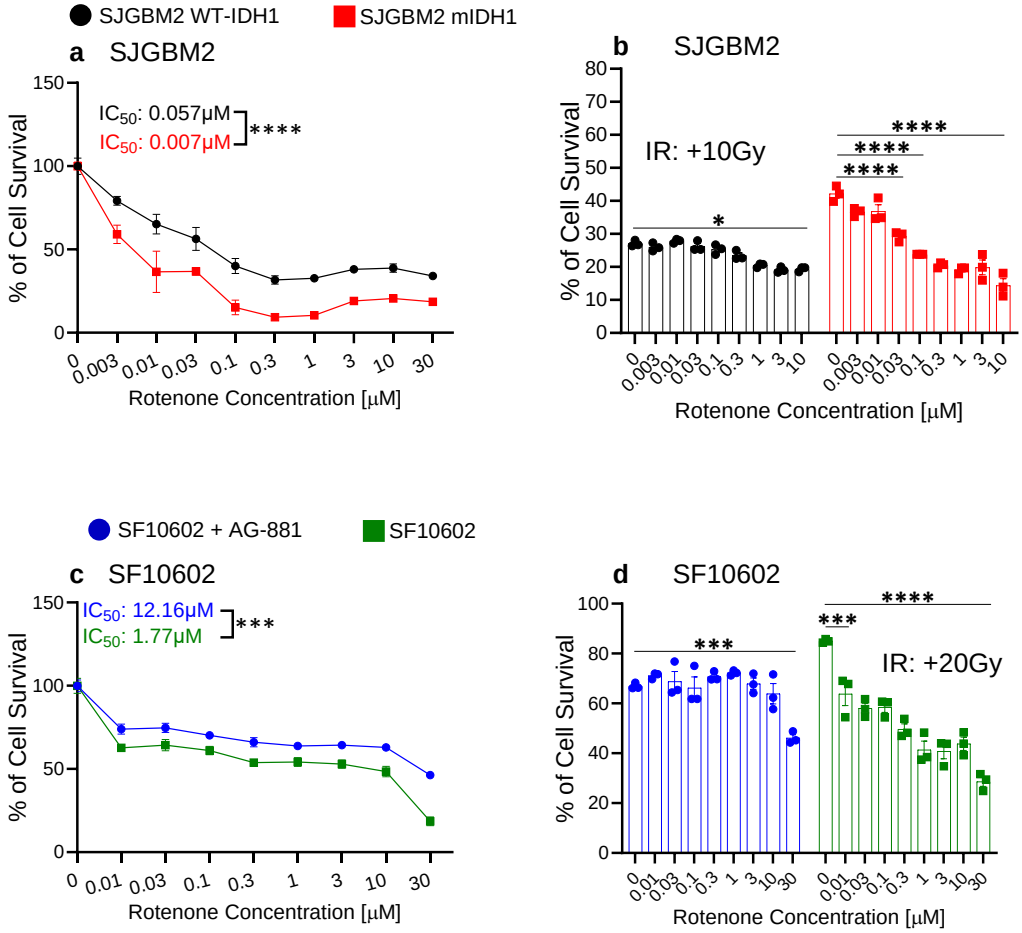

Supplementary Figure 10: *In vitro* inhibition of Complex I of the ETC induces cell death and restores radiosensitivity in two human mIDH1 glioma cells. (**a**) Cell viability assay of WT-IDH1 and mIDH1 genetically engineered human glioma cells, SJGBM2, treated with rotenone for 72 hours at increasing concentrations. Cell viability expressed as % of cell survival relative to control populations. A linear regression model and generalized additive models were used to determine the dose-response relationship. (**b**) Cell viability assay showing the effect of rotenone at increasing concentrations in combination with radiation (10Gy) on the proliferation of WT-IDH1 and mIDH1 SJGBM2 cells. (**c**) Cell viability assay of endogenous mIDH1 glioma cells, SF10602, treated with and without mIDH1 inhibitor, AG-881, were treated with rotenone for 72 hours at increasing concentrations. Cell viability expressed as % of cell survival relative

to control populations. A linear regression model and generalized additive models were used to determine the dose-response relationship. (**d**) Cell viability assay showing the effect of rotenone at increasing concentrations in combination with radiation (20Gy) on the proliferation of AG-881 treated SF10602 and untreated SF10602 cells. Results are expressed as % of Cell survival relative to control populations. Statistical analyses were conducted using student's t-test and error bars depict SD of technical replicates from 3 independent experiments. *$P < 0.1$, **$P < 0.01$, ***$P < 0.001$, ****$P < 0.0001$, ns = not significant.

Supplementary Figure 11: Densitometric analysis of western blots shown in Figure 6.

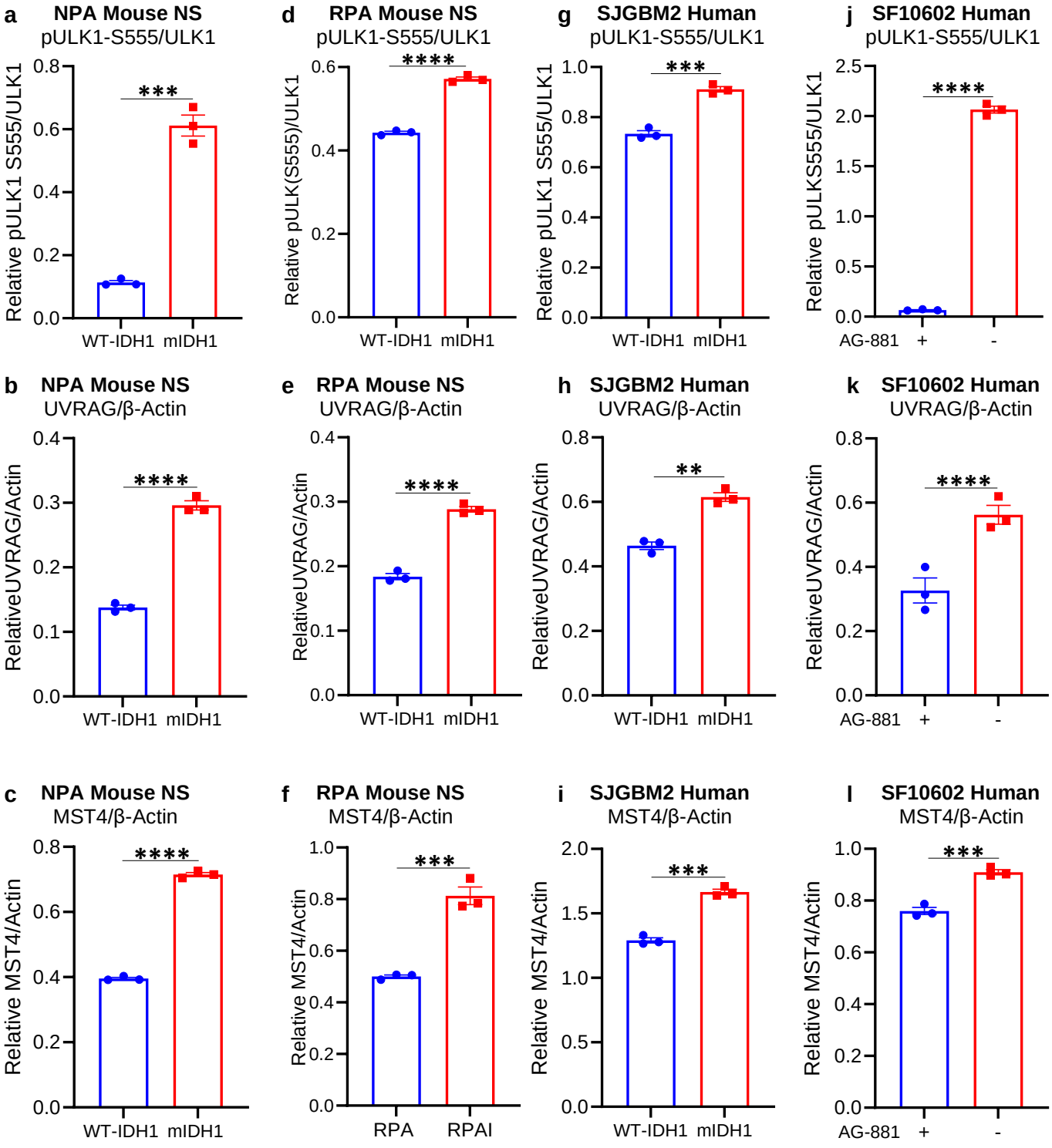

1 **Supplementary Figure 11: Densiometric analysis of western blots shown in Figure 6.**

2 Densiometric analysis of (**a-c**) NPA Mouse NS, (**d-f**) RPA Mouse NS, (**g-i**) SJGBM2 cells,

3 and (**j-l**) SF10602 cells ± AG-881 Western blots. ImageJ densitometric quantification of the

western blots of pULK1-S555 (a, d, g, j), UVRAG (b, e, h, k), and MST4 (c, f, i, l). Errors bars represent SEM from independent technical replicates (n = 3). ***$P < 0.001$; ****$P < 0.0001$; unpaired t test.

Supplementary Figure 12: Autophagy flux assay using a lentivirus to express LC3 protein associated with GFP and mCherry reporter protein.

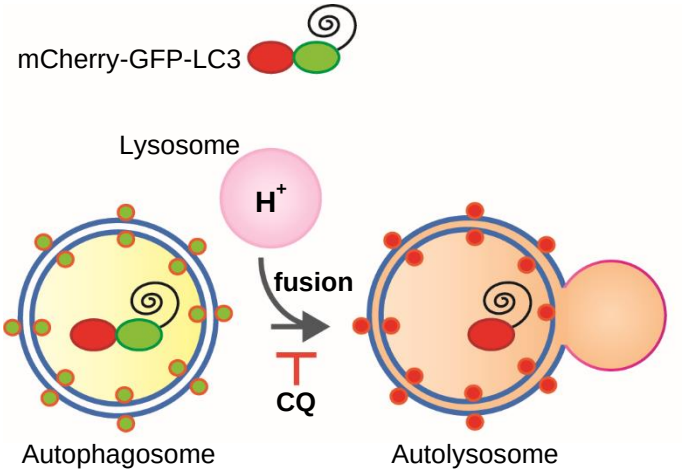

Supplementary Figure 12: Autophagy flux assay using a lentivirus to express LC3 protein associated with GFP and mCherry reporter protein. In cells expressing mCherry-GFP-LC3, autophagosomes display both GFP and mCherry fluorescence, whereas autolysosomes display only mCherry fluorescence (red) because GFP is denatured by the acidity of the lysosome. Chloroquine (CQ) inhibits the fusion step in autophagy flux, disrupting autolysosome formation.

Supplementary Figure 13: Validation of ATG4b, ATG7, and ATG9b siRNAs.

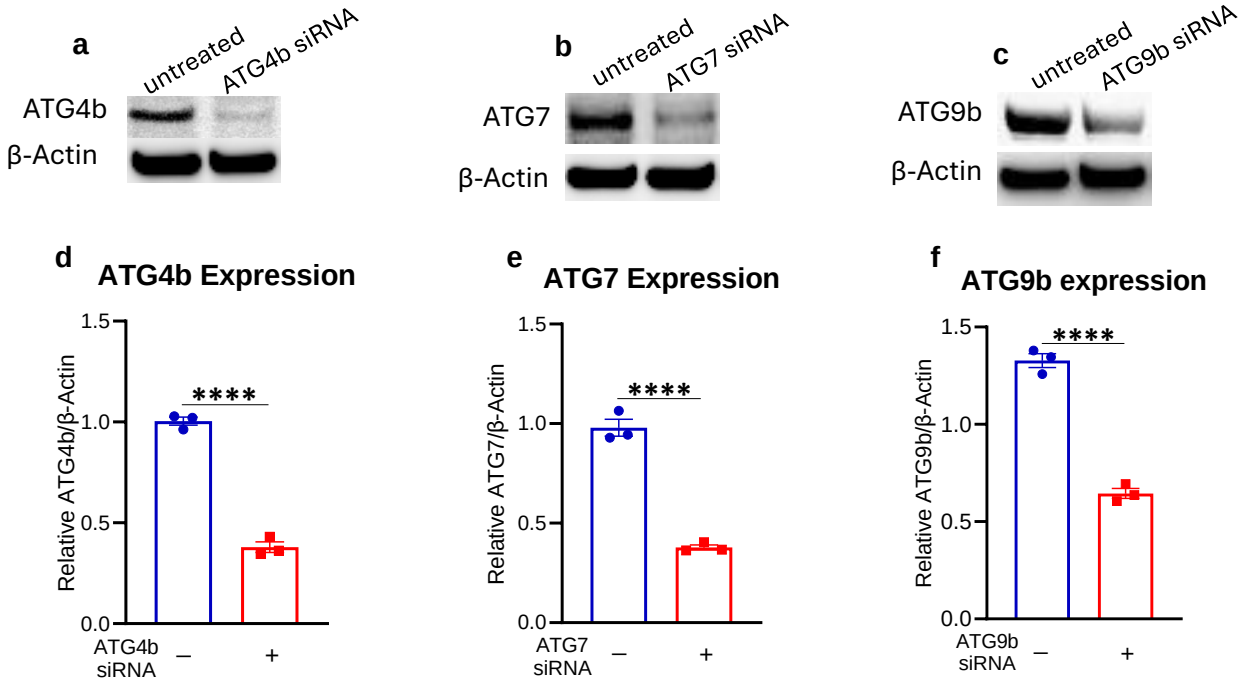

Supplementary Figure 13: Validation of ATG4b, ATG7, and ATG9b siRNAs. (**a-c**) Western blot analysis showing successful inhibition of (a) ATG4b, (b) ATG7, and (c) ATG9b via siRNA in mIDH1 NPA mouse glioma NS (NPAI) with β-actin as a loading control. (**d-f**) ImageJ densitometric quantification of the western blot for (d) relative ATG4b/β-actin, (e) relative ATG7/β-actin, and (f) relative ATG9b/β-actin. Errors bars represent SEM from independent biological replicates (n = 3). ****$P < 0.0001$; unpaired t test.

Supplementary Figure 14: Silencing autophagy induces cytotoxicity and restores radiosensitivity in two genetically engineered mouse glioma cell models: RPAI and CPAI.

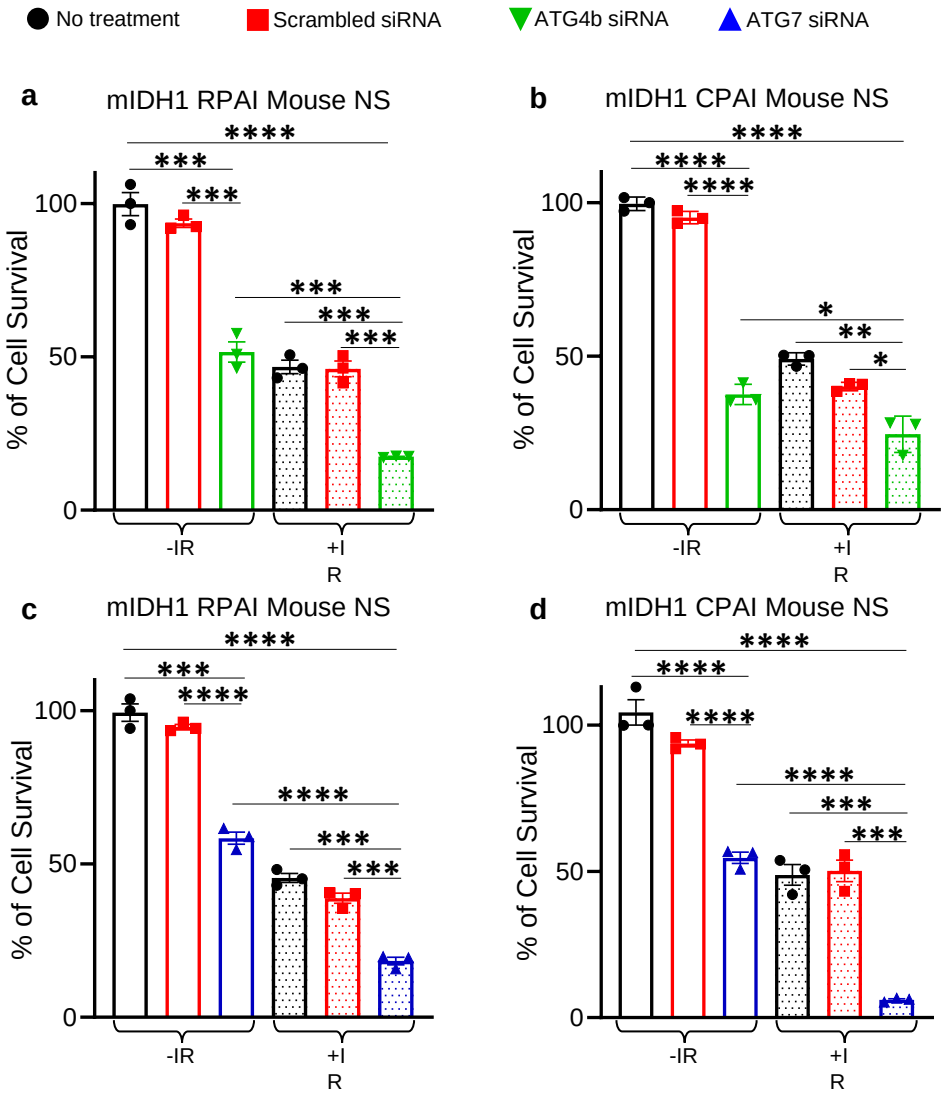

Supplementary Figure 14: Silencing autophagy induces cytotoxicity and restores radiosensitivity in two genetically engineered mouse glioma cell models: RPAI and CPAI. Cell Titer Glo assays (luminescence) show the impact of (**a-b**) ATG4b silencing (ATG4b siRNA) and (**c-d**) ATG7 silencing (ATG7 siRNA) on cellular cytotoxicity and radiosensitivity on (a, c) mIDH1 RPAI mouse NS, (b, d) mIDH1 CPAI mouse NS. Cells were treated with saline, scrambled siRNA, free ATG4b siRNAs (a-b), or free ATG7 siRNAs (c-d). The amount of ATG4b siRNA or ATG7 siRNA used was 100 nM. The amount of radiation used was 3 Gy. All experiments were performed in quadruplicate, and results are expressed as "% cell survival". Statistical analyses were conducted using student's t test and error bars depicting the

SEM of technical replicates from 3 independent experiments. *$P < 0.1$, **$P < 0.01$, ***$P < 0.001$, ****$P < 0.0001$.

Supplementary Figure 15: Silencing autophagy induces cytotoxicity and restores radiosensitivity in both patient-derived glioma cells and genetically engineered mouse glioma cells.

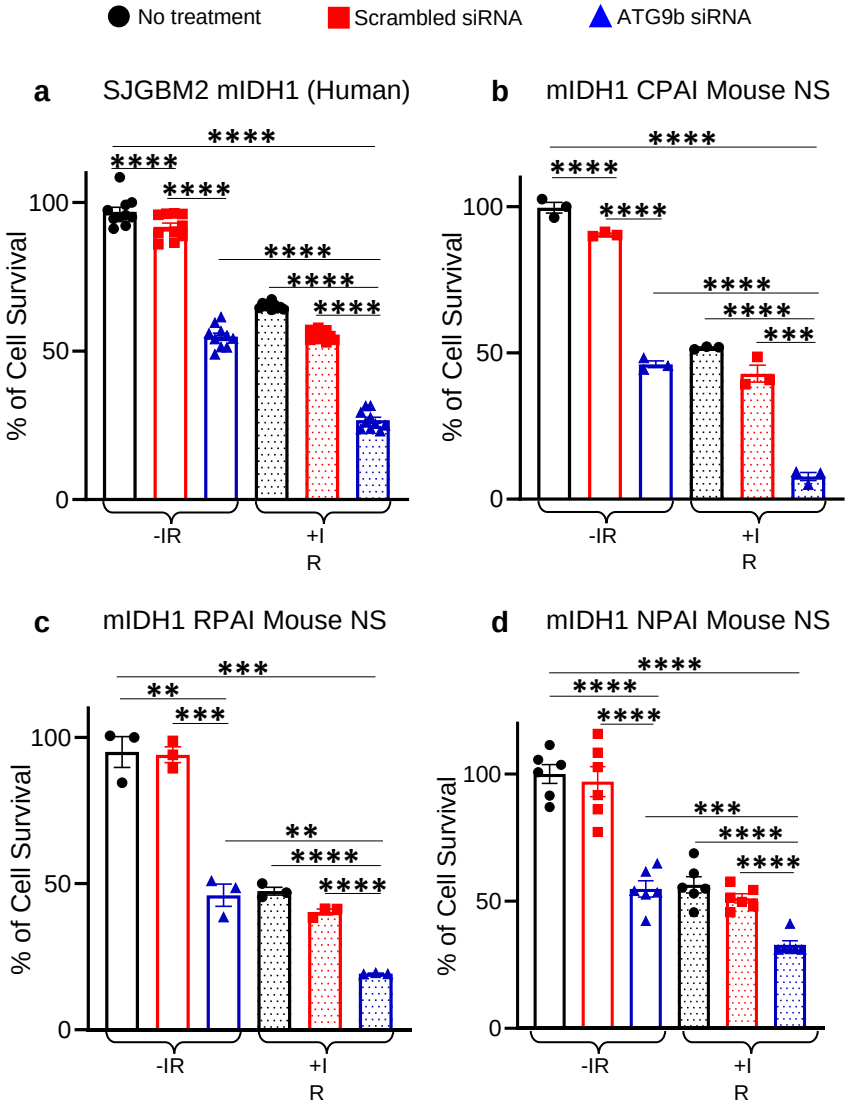

Supplementary Figure 15: Silencing autophagy induces cytotoxicity and restores radiosensitivity in both patient-derived glioma cells and genetically engineered mouse glioma cells. Cell Titer Glo assays (luminescence) show the impact of ATG9b silencing (ATG9b siRNA) on cellular cytotoxicity and radiosensitivity on (**a**) SJGBM2 mIDH1 human cells, (**b**) mIDH1 CPAI mouse NS, (**c**) mIDH1 RPAI mouse NS, and (**d**) mIDH1 NPAI mouse NS. Cells were treated with saline, scrambled siRNA, or free ATG9b siRNA. The amount of ATG9b siRNA used was 100nM for all mouse cells and 150nM for all human cells. The amount of radiation used was 5 Gy for SJGBM2 cells and 3 Gy for mouse NS. All experiments were performed in quadruplicate, and results are expressed as "% cell survival". Statistical analyses

were conducted using student's t test and error bars depicting the SEM of technical replicates from 3 independent experiments. $^{**}P < 0.01$, $^{***}P < 0.001$, $^{****}P < 0.0001$.

Supplementary Figure 16: Generation of autophagy deficient mIDH1 mouse glioma cells.

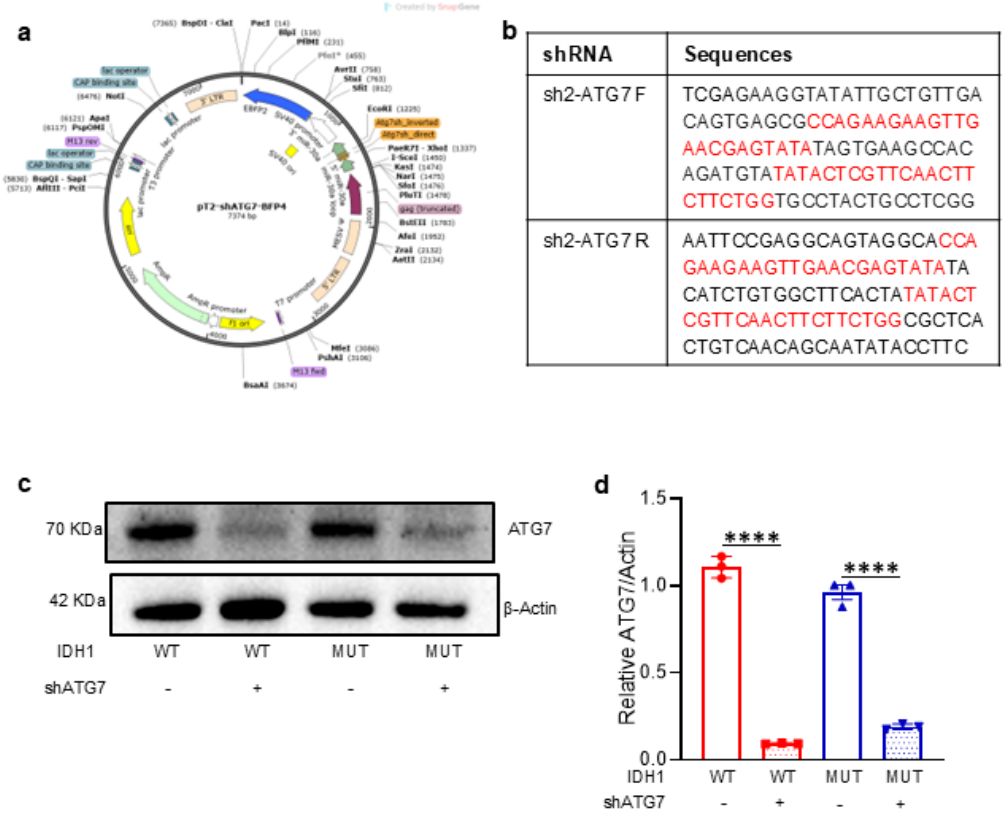

Supplementary Figure 16: Generation of autophagy deficient mIDH1 mouse glioma cells. (**a**) Sleeping Beauty (SB) plasmid pT2-shATG7-BFP4, containing a short hairpin targeting in *Atg7*, was used for *in vitro* and in vivo knockdown of *Atg7* expression in mIDH1 glioma using the SB transposon system. The plasmid map illustrates the final construction, which encodes for shATG7 (HP_603911) and enhanced blue fluorescent protein (EBFP). (**b**) Corresponding shRNA sequences highlighted in red for shAtg7. (**c, d**) Western blot analysis showing successful knockdown of ATG7 within wtIDH1 cells (WT) and mIDH1 cells (MUT) with β-actin as a loading control. ImageJ densitometric quantification of the western blot for ATG7 and β-actin. Errors bars represent SEM from independent biological replicates (n = 3). ****$p < 0.0001$; unpaired t test.

Supplementary Figure 17: Silencing autophagy restores radiosensitivity in mIDH1 mouse NS.

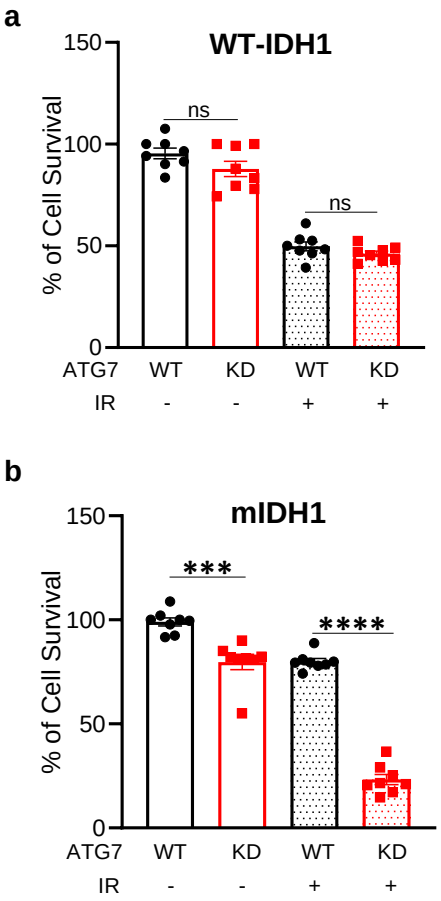

Supplementary Figure 17: Silencing autophagy restores radiosensitivity in mIDH1 mouse NS. Cell proliferation assays show the impact of ATG7 knockdown (ATG7 KD) on radiosensitivity in (**a**) NRAS/shP53/shATRX (NPA) mouse NS and (**b**) NRAS/shP53/shATRX/mIDH1 (NPAI) mouse NS, when treated with 3 Gy of radiation. All the experiments were performed in octuplicate (8 replicates), and the results are expressed in "% cell survival". Statistical analyses were done with student's t test and error bars depicting the SD of technical replicates from 3 independent experiments. ***$P < 0.001$, ****$P < 0.0001$, ns = not significant.

Supplementary Figure 18: Cytokine profiling in mIDH1 glioma mouse NS in response to autophagy inhibition and IR.

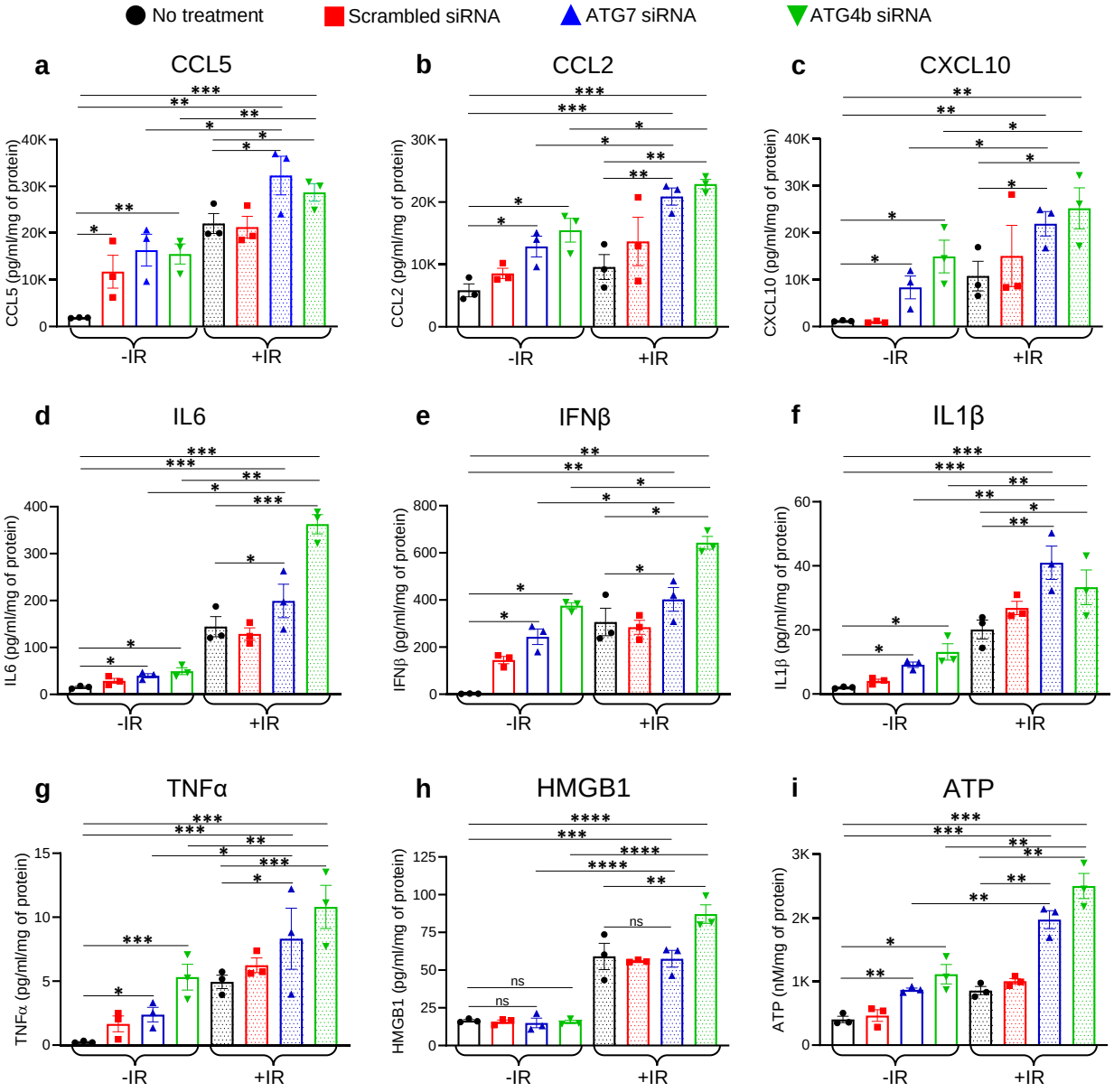

Supplementary Figure 18: Cytokine profiling in mIDH1 glioma mouse NS in response to autophagy inhibition and IR. The following cytokines were profiled in mIDH1 glioma mouse NS in response to autophagy inhibition and IR: Levels of DAMPs and Type-I IFNs i.e. (**a**) CCL5; (**b**) CCL2; (**c**) CXCL10; (**d**) IL6; (**e**) IFNβ; (**f**) IL1β; (**g**) TNFα; (**h**) HMGB1; and (**i**) ATP were determined through ELISA following treatment with 100nM of ATG7 and ATG4b siRNAs in combination with 3Gy ionizing radiation (IR). Conditioned media were collected and analyzed after 72h post-treatment. Statistical significances were determined using one-way

ANOVA followed by Tukey's test. Significances denoted as follows: *$P < 0.05$, **$P < 0.01$, ***$P < 0.001$, ****$P < 0.0001$, ns = not significant. The bars represent the mean ± SEM (n = 3 biological replicates).

Supplementary Figure 19: Cytokine profiling in mIDH1 SJGBM2 cells in response to autophagy inhibition and IR.

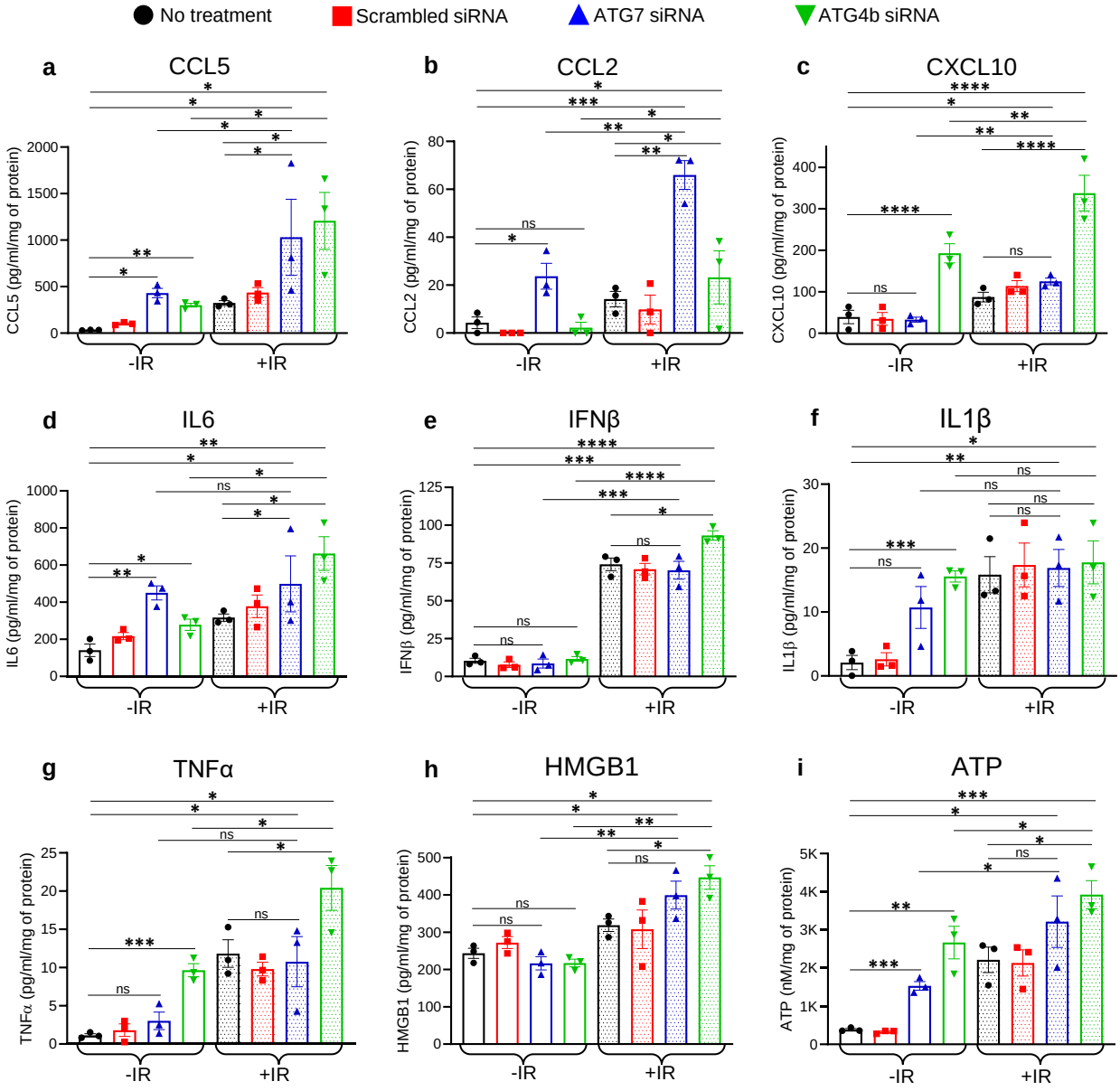

Supplementary Figure 19: Cytokine profiling in mIDH1 SJGBM2 cells in response to autophagy inhibition and IR. The following cytokines were profiled in human mIDH1 glioma cells in response to autophagy inhibition and IR: Levels of DAMPs and Type-I IFNs i.e. (**a**) CCL5; (**b**) CCL2; (**c**) CXCL10; (**d**) IL6; (**e**) IFNβ; (**f**) IL1β; (**g**) TNFα; (**h**) HMGB1; and (**i**) ATP were determined through ELISA following treatment with 150nM of ATG7 and ATG4b siRNAs in combination with 5Gy IR. Conditioned media were collected and analyzed after 72h post-treatment. Statistical significances were determined using one-way ANOVA

followed by Tukey's test. Significances denoted as follows: *P < 0.05, **P < 0.01, ***P < 0.001, ****P < 0.0001, ns = not significant. The bars represent the mean ± SEM (n = 3 biological replicates).

Supplementary Figure 20: Sleeping beauty plasmid pT2-shATG7-EGFP.

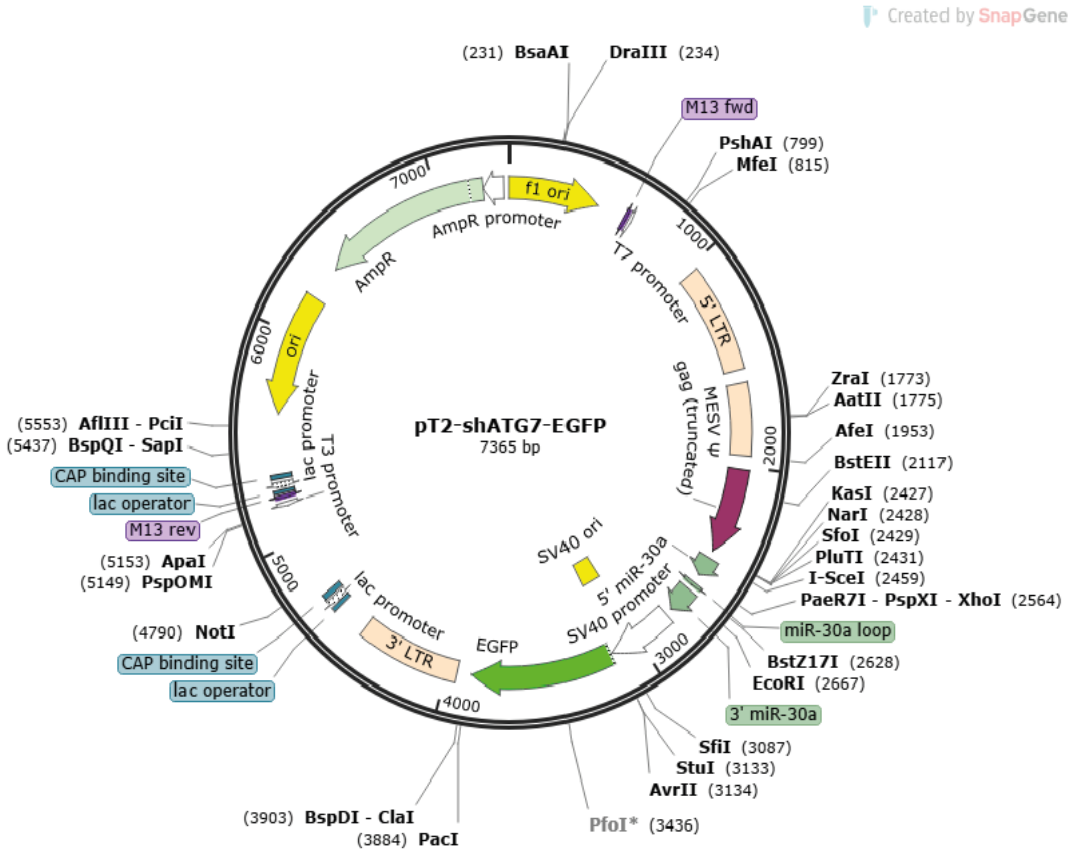

shATG7 (HP_603911):

CTCGAGTGCTGTTGACAGTGAGCGACCAGAAGAAGTTGAACGAGTATAGTGAAGCCACAGATGTATACTCTTCAACTTCTTT
GGGTGCCTACTCCTCGGAGAATTC

1

2 **Supplementary Figure 20: Sleeping beauty plasmid pT2-shATG7-EGFP.** Generation of an
3 autophagy deficient mIDH1 mouse glioma model. Sleeping Beauty (SB) plasmid pT2-shAtg7-
4 GFP, containing a short hairpin targeting in *Atg7*, was used for in vivo knockdown of *Atg7*
5 expression in mIDH1 glioma using the SB transposon system. The plasmid map illustrates the
6 final construction, which encodes for shATG7 (HP_603911) and EGFP.

7

Supplementary Figure 21: ATG7i-SPNP fabrication and characterization.

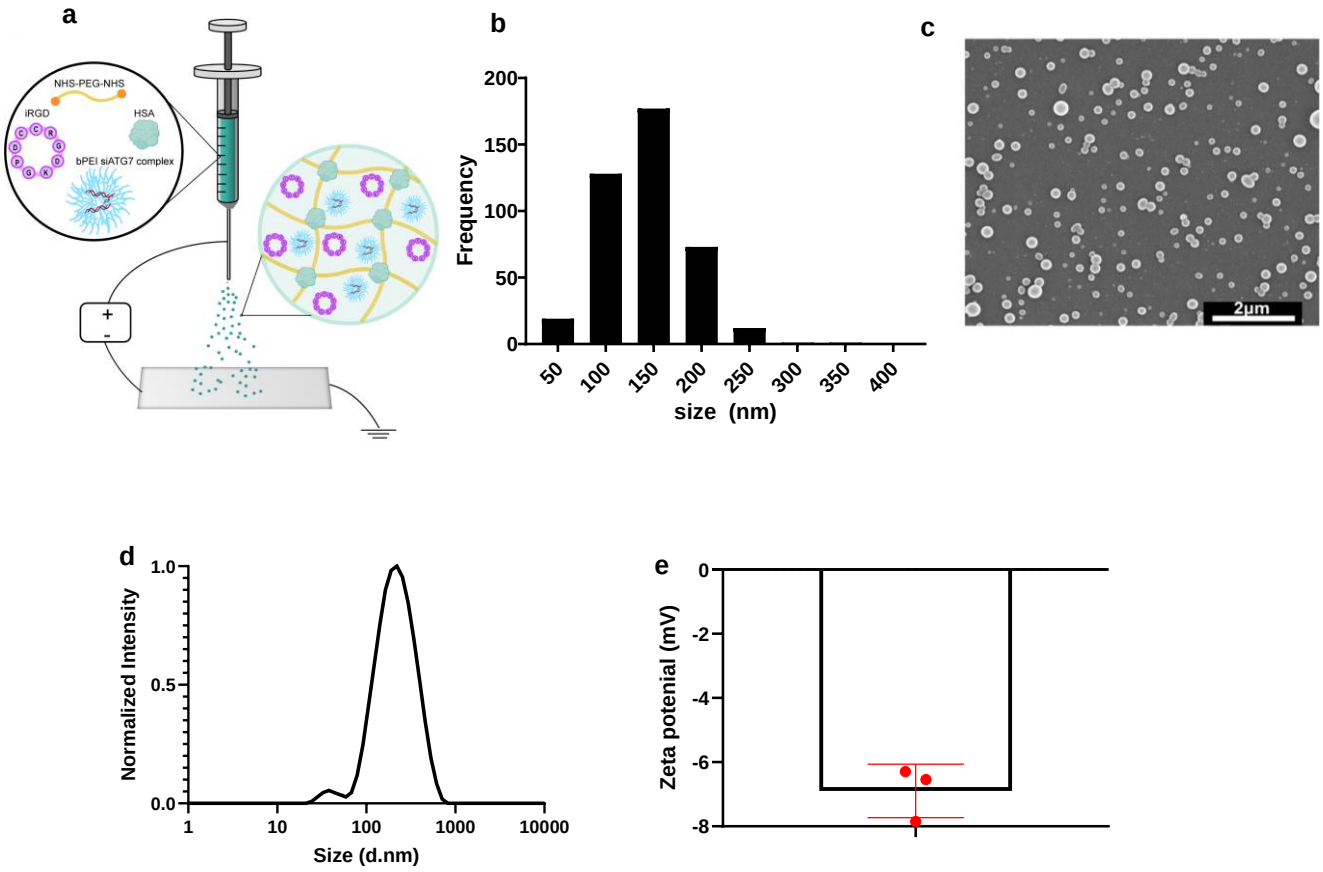

Supplementary Figure 21: ATG7i-SPNP fabrication and characterization. (**a**) Electrohydrodynamic jetting to produce ATG7i-SPNPs. All components (lysine-containing iRGD, branched PEI-siATG7 complex, PEG crosslinker, BSA Alexa Fluor 647 conjugate) are added in the initial solution. Solid SPNPs result on the plate and are crosslinked for 7 days. (**b**) Histogram of dry state SPNP diameter (mean diameter: 104 ± 42 nm) analyzed from Scanning Electron Microscopy of n > 400 individual SPNPs. (**c**) Scanning electron microscopy micrograph (scale bar = 2 µm). (**d**) Intensity-based dynamic light scattering spectra ($Z_{average}$=185 nm, peak diameter = 238 nm, PDI = 0.289). (**e**) Zeta potential (-6.84 ± 0.69 mV).

Supplementary Figure 22: Batch to batch production of ATG7i-SPNPs.

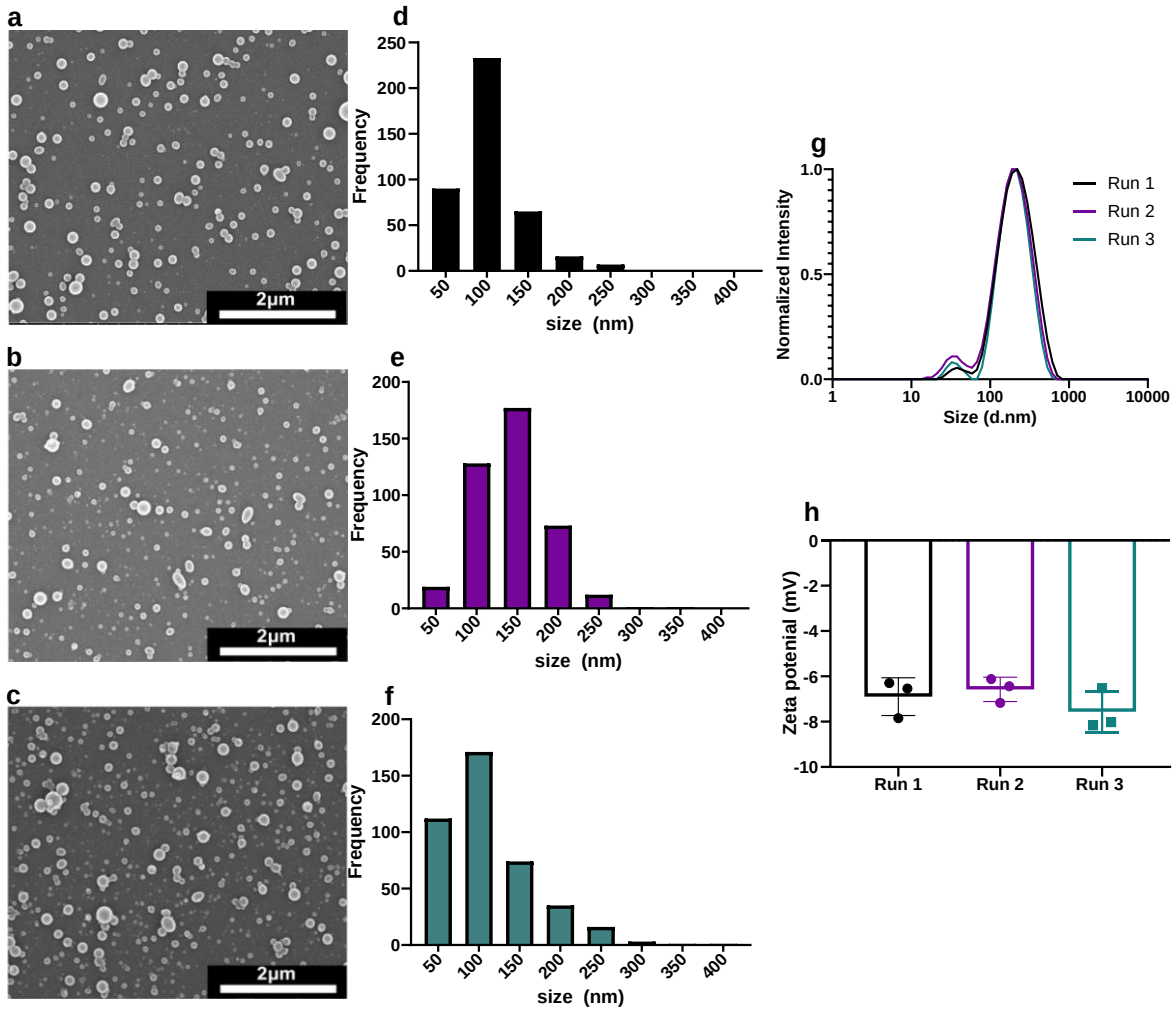

Supplementary Figure 22: Batch to batch production of ATG7i-SPNPs. Comparison of ATG7i-SPNPs characteristics that were fabricated and collected in three independent sessions. (**a-f**) A scanning electron microscope image (a-c) and the corresponding histogram (d-f) of the size distribution in the dry state of (a, d) run 1, (b, e) run 2, and (c, f) run 3. (**g**) Intensity dynamic light scattering spectra post-collection of the three runs. (**h**) Zeta potential.

Supplemental Figure 23: Silencing autophagy using ATG7i-SPNPs induces cytotoxicity and restores radiosensitivity in genetically engineered mouse glioma cells.

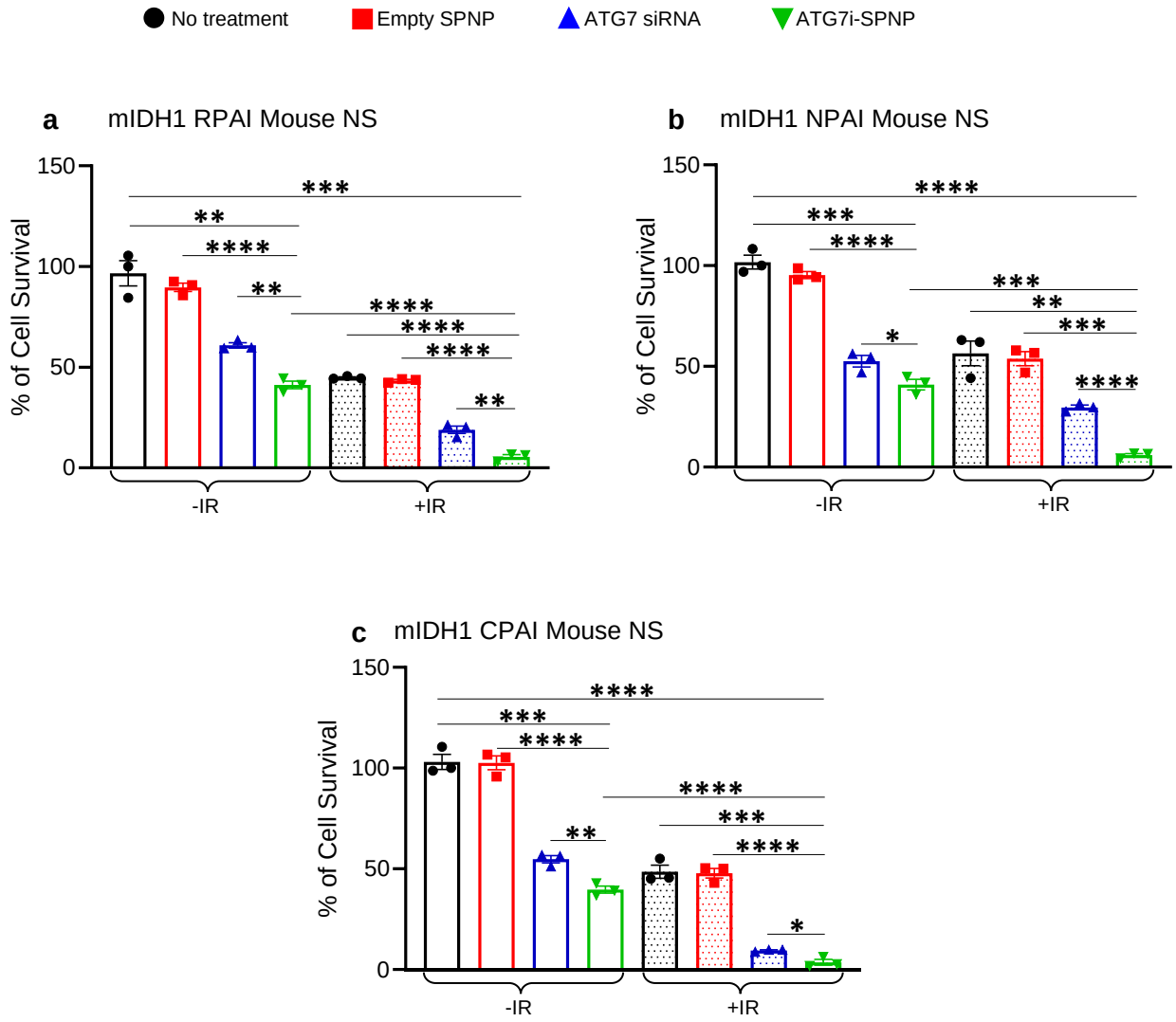

Supplementary Figure 23: Silencing autophagy using ATG7i-SPNPs induces cytotoxicity and restores radiosensitivity in genetically engineered mouse glioma cells. Cell Titer Glo assays (luminescence) show the impact of ATG7 silencing (ATG7 siRNA) on cellular cytotoxicity and radiosensitivity in (**a**) mIDH1 RPAI mouse NS, (**b**) mIDH1 NPAI mouse NS, and (**c**) mIDH1 CPAI mouse NS. Cells were treated with saline, empty nanoparticles (SPNPs), free ATG7 siRNAs, and ATG7 siRNA loaded nanoparticles (ATG7i-SPNPs). The amount of ATG7 siRNA used or loaded in the nanoparticle was 25µg. The amount of radiation used was 3 Gy. All experiments were performed in quadruplicate, and results are expressed as "% cell survival". Statistical analyses were conducted using student's t test and error bars depicting the

SEM of technical replicates from 3 independent experiments. *P < 0.1, **P < 0.01, ***P < 0.001, ****P < 0.0001.

Supplementary Figure 24: Silencing autophagy using ATG7i-SPNPs induces cytotoxicity and restores radiosensitivity in mIDH1 human genetically engineered and patient-derived glioma cells.

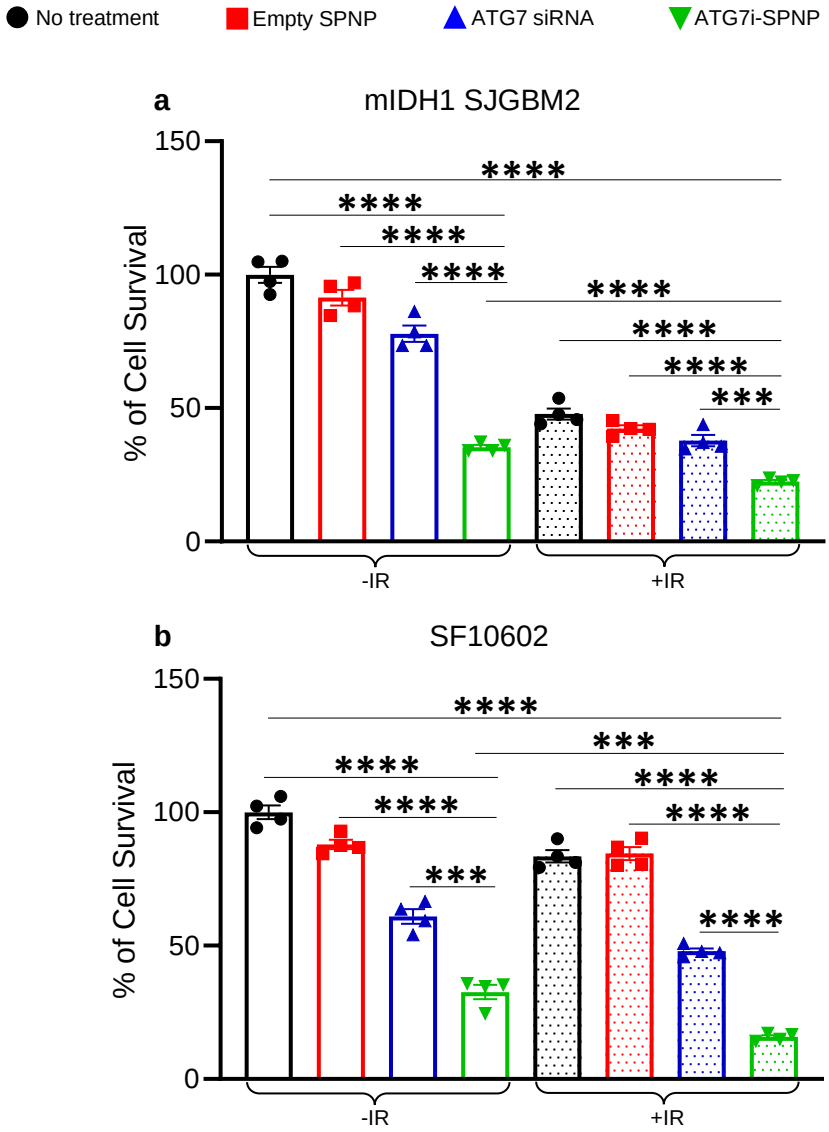

Supplementary Figure 24: Silencing autophagy using ATG7i-SPNPs induces cytotoxicity and restores radiosensitivity in mIDH1 human genetically engineered and patient-derived glioma cells. Cell Titer Glo assays (luminescence) show the impact of ATG7 silencing (ATG7 siRNA) on cellular cytotoxicity and radiosensitivity in (**a**) mIDH1 SJ-GBM2 following treatment with 10 Gy of irradiation. Similarly, the same luminescence assay was performed to evaluate the effect of ATG7 silencing on cellular cytotoxicity and radiosensitivity in (**b**) endogenous mIDH1-expressing human SF10602 cells, following 20 Gy of irradiation. Cells were treated with saline, empty nanoparticles (SPNPs), free ATG7 siRNAs, and ATG7 siRNA

loaded nanoparticles (ATG7i-SPNPs). The amount of ATG7 siRNA used or loaded in the nanoparticle was 25µg. All experiments were performed in quadruplicate, and results are expressed as "% cell survival". Statistical analyses were conducted using student's t test and error bars depicting the SEM of technical replicates from 3 independent experiments. ***$P <$ 0.001, ****$P < 0.0001$.

Supplementary Figure 25: Evaluation of brain and liver histopathology at an early time point following ATG7i-SPNP treatment in combination with IR in mIDH1 glioma-bearing mice.

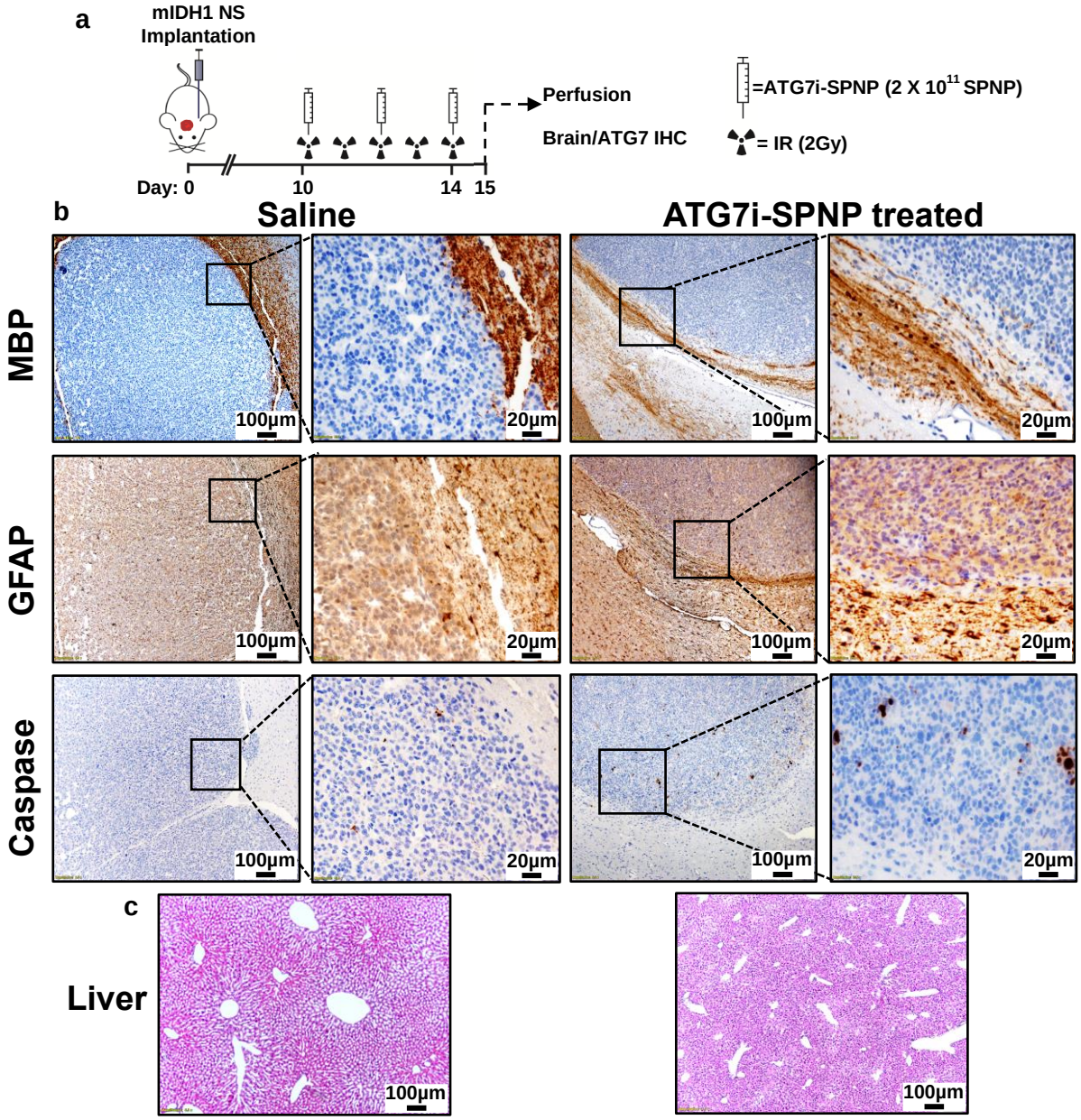

Supplementary Figure 25: **Evaluation of brain and liver histopathology at an early time point following ATG7i-SPNP treatment in combination with IR in mIDH1 glioma-bearing mice.** (**a**) Schematic of experimental design for the 14-day timed experiment: mIDH1 NS were implanted intracranially on Day 0. Mice were treated with ATG7i-SPNP on days 10, 12, and 14. Subsequently, mice were perfused at the end of Day 14 and analyzed. (**b**) Representative Immunohistochemical (IHC) staining of 5 µm paraffin-embedded brain sections from saline and ATG7i–SPNP treated groups, stained for MBP (myelin basic protein),

GFAP (glial fibrillary acidic protein), and cleaved Caspase-3. MBP and GFAP staining are markers for regional demyelination and astrogliosis, respectively. Increased cleaved Caspase-3 staining in treated brains suggests enhanced apoptosis. Low magnification (10×) panels (black scale bar = 100 μm), High magnification (40×) panels (black scale bar = 20 μm) indicate positive staining for the areas in the low-magnification panels (**c**) Representative H&E-stained liver sections from both groups show no histopathological abnormalities, suggesting no systemic toxicity due to ATG7i-SPNP treatment.

Supplementary Figure 26: Long-term survivors were rechallenged with genetically engineered mIDH1 mouse glioma NS.

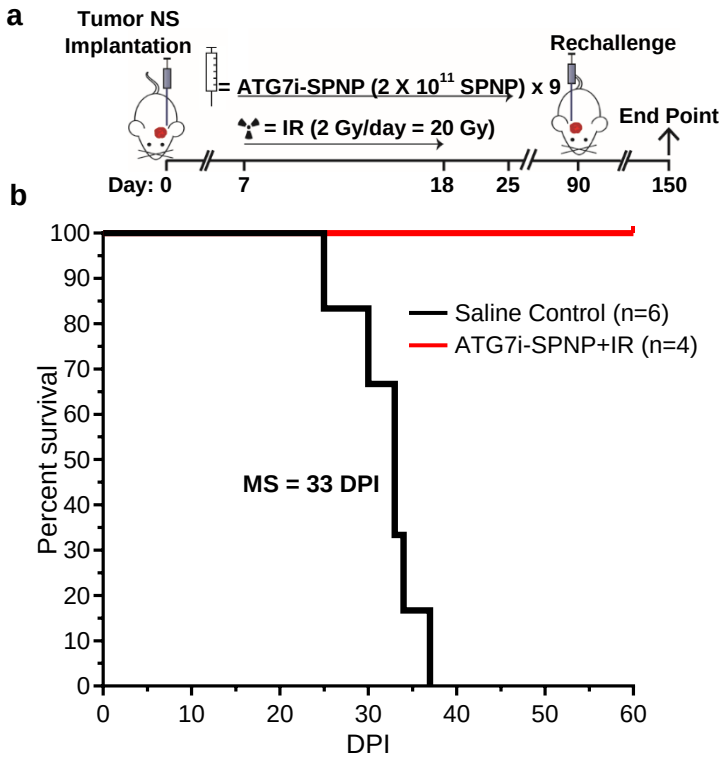

Supplementary Figure 26: Long-term survivors were rechallenged with genetically engineered mIDH1 mouse glioma NS. (**a**) Experimental design detailing when mice treated with ATG7i-SPNPs were considered long-term survivors, at which point they were rechallenged. (**b**) Kaplan-Meier curve showing the survival of long-term survivor mice that were rechallenged with genetically engineered mouse mIDH1 glioma NS.

Supplementary Figure 27: Histopathological assessment of livers from tumor bearing mice treated with ATG7i-SPNPs + IR.

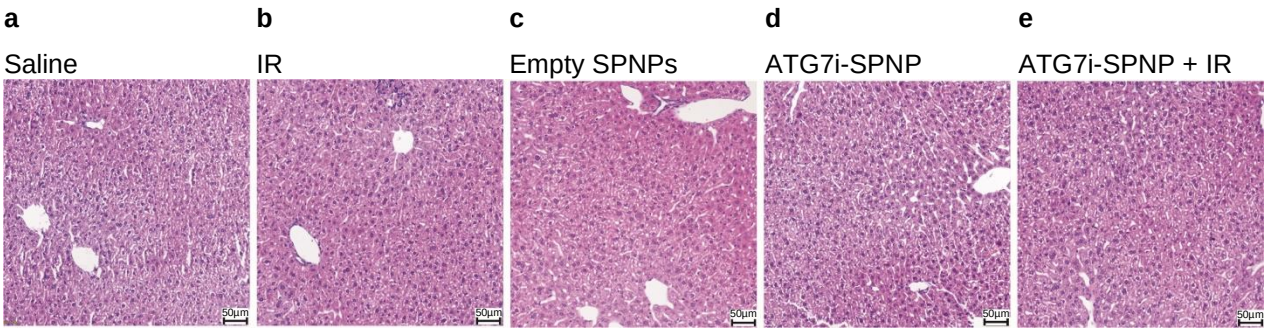

Supplementary Figure 27: Histopathological assessment of livers from tumor bearing mice treated with ATG7i-SPNPs + IR. H&E staining of 5µm paraffin embedded liver sections from (**a**) Saline (20X), (**b**) IR (20X), (**c**) empty SPNPs (20X), (**d**) ATG7i-SPNPs (20X) and (**e**) ATG7i-SPNP + IR (20X) treatment groups. Histology performed on resected livers following complete treatment of NPAI tumor bearing mice. Representative images from an experiment consisting of independent biological replicates are displayed. Black scale bars = 50µm.

Supplementary Figure 28: Mouse serum biochemical analysis following intravenous ATG7i-SPNP in combination with IR treatment.

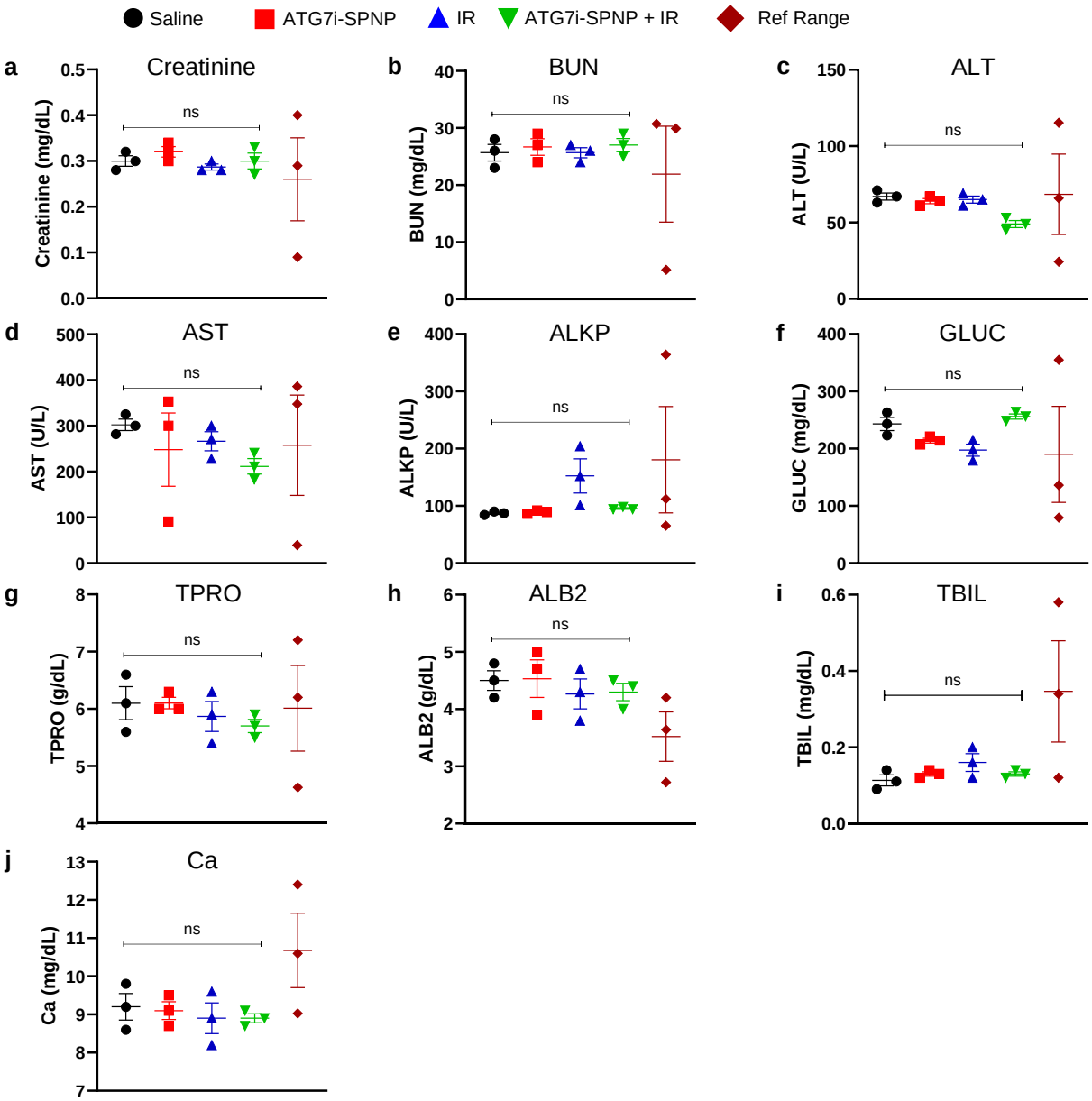

Supplementary Figure 28: Mouse serum biochemical analysis following intravenous ATG7i-SPNP in combination with IR treatment. NPAI OVA tumor bearing mice treated with ATG7 inhibitor ATG7i-SPNPs in combination with IR exhibit normal serum biochemical parameters compared with saline treated control. Serum was collected from tumor bearing mice treated with saline, ATG7i-SPNPs, IR, or ATG7i-SPNP + IR at 23 DPI. For each treatment group levels of (**a**) Creatinine, (**b**) BUN, (**c**) ALT, (**d**) AST, (**e**) ALKP, (**f**) GLUC, (**g**) TPRO, (**h**) ALB2, (**i**) TBIL, and (**j**) Ca were quantified. The levels of different serum biochemical

parameters between the treatment groups were compared and were found non-significant (n = 3 biological replicates).

Supplementary Figure 29: ATG7i-SPNP treatment + IR leads to enhanced T cell proliferation and activation in response to SIINFEKL stimulation and splenocytes.

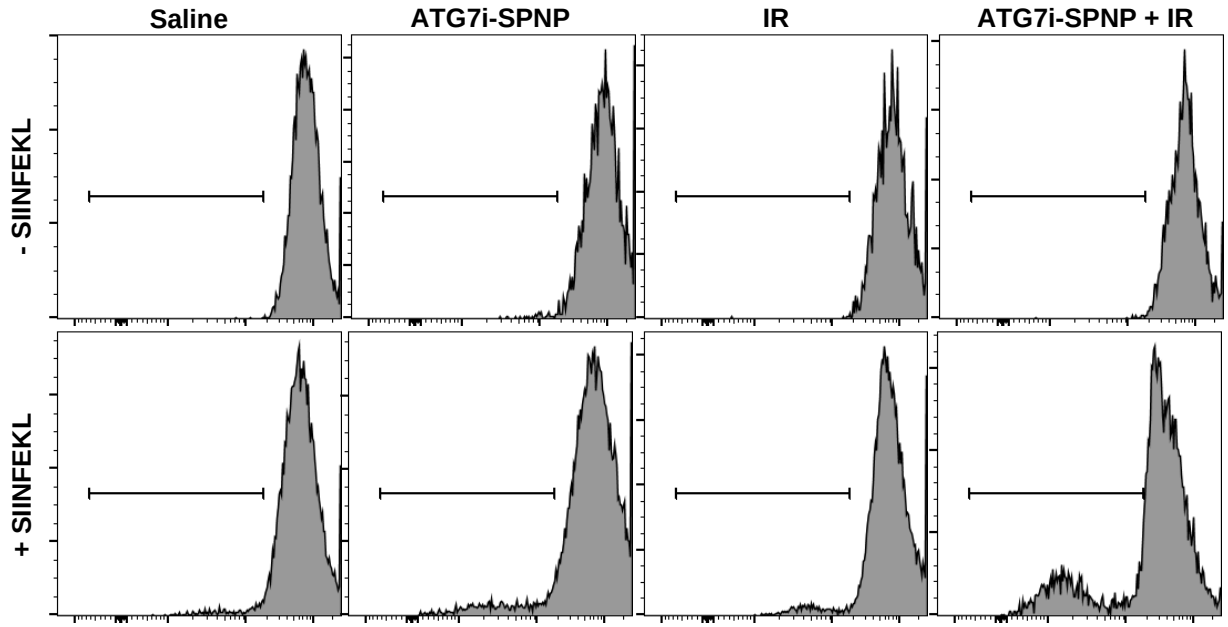

Supplementary Figure 29: ATG7i-SPNP treatment + IR leads to enhanced T cell proliferation and activation in response to SIINFEKL stimulation of splenocytes. T cell proliferation was measured as the reduction of CFSE staining in the CD45+/CD3+/CD8+ population. Upper panel: Representative histograms show CFSE stains of unstimulated splenocytes (inactivated T cells) and Lower panel: Representative histograms show 100nM SIINFEKL-induced T cell proliferation from Saline, ATG7i-SPNP, IR and ATG7i-SPNP + IR treated groups.

Supplementary Figure 30: Histopathological assessment of brains from tumor bearing mice treated with ATG7i-SPNP + IR.

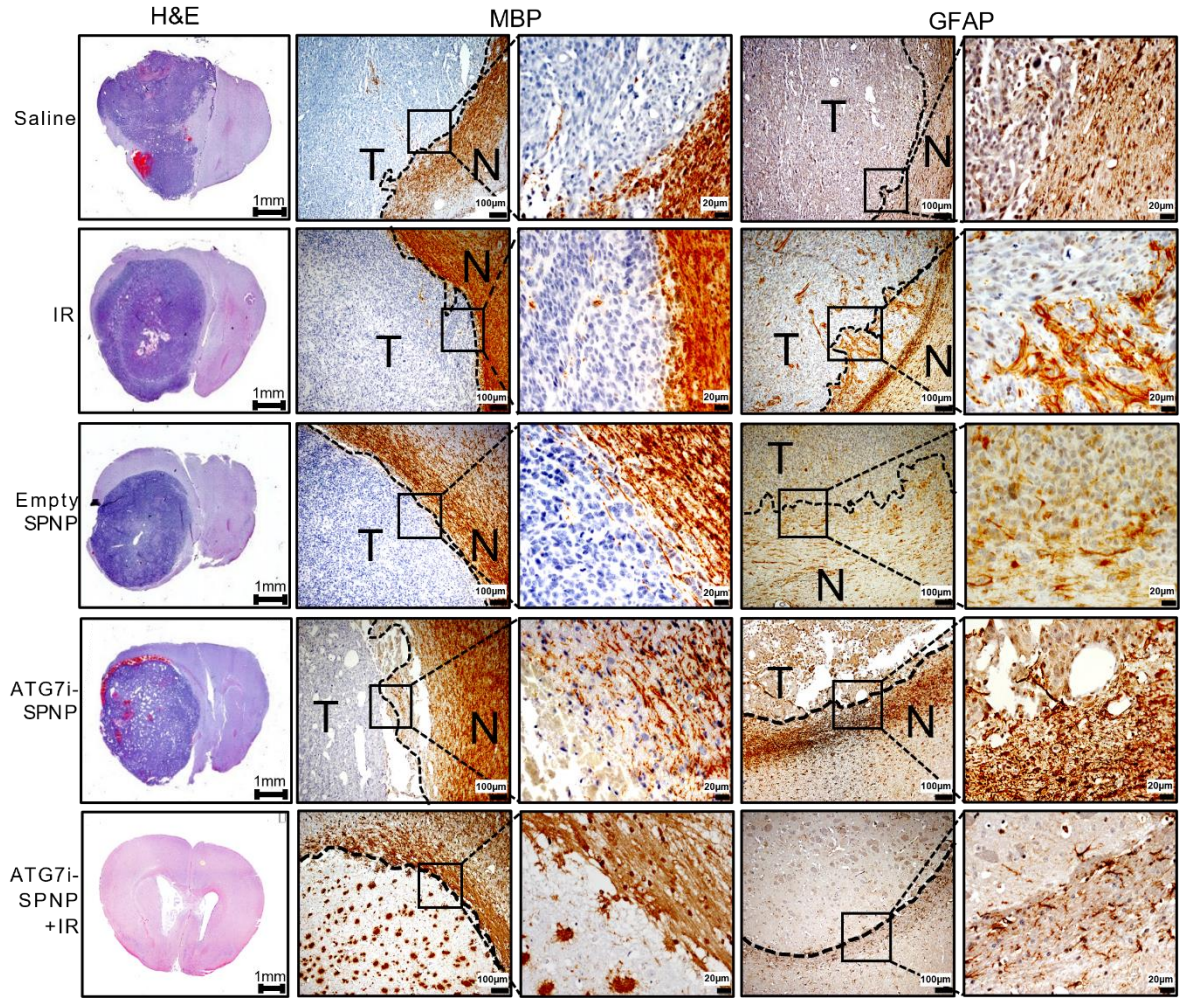

Supplementary Figure 30: Histopathological assessment of brains from tumor bearing mice treated with ATG7i-SPNP + IR. H&E staining of 5µm paraffin embedded brain sections from saline, IR, Empty SPNP, ATG7i-SPNP, and long-term survivors from ATG7i-SPNP+IR treatment groups (scale bar=1mm). Paraffin embedded 5µm brain sections for each treatment group were stained for myeline basic protein (MBP), and glial fibrillary acidic protein (GFAP). Low magnification (10X) panels show normal brain (N) and tumor (T) tissue (black scale bar = 100 µm). High magnification (40X) panels (black scale bar = 20 µm) indicate positive staining for areas delineated in low-magnification panels. Representative images from a single experiment consisting of independent biological replicates are displayed.

Supplementary Figure 31: Histopathological assessment of brains from tumor bearing mice treated with ATG7i-SPNP + IR.

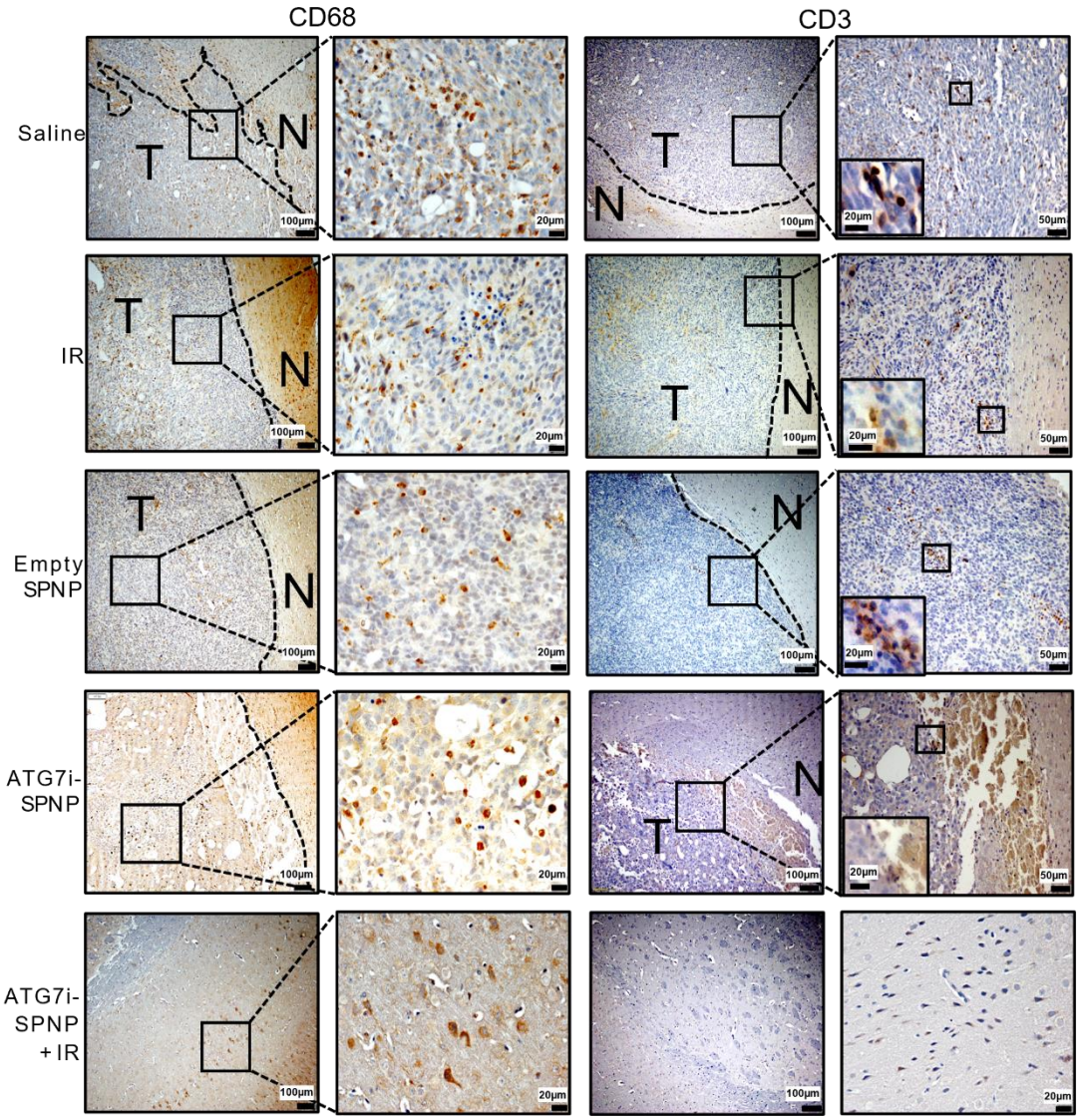

Supplementary Figure 31: Histopathological assessment of brains from tumor bearing mice treated with ATG7i-SPNP + IR. Paraffin embedded 5μm brain sections of the following treatment groups: saline, IR, Empty SPNP, ATG7i-SPNP, and long-term survivors from ATG7i-SPNP+IR were stained for CD68 and CD3. Low magnification (10X) panels show normal brain (N) and tumor (T) tissue (black scale bar = 100 μm). High magnification (40X) panels (black scale bar = 50 μm for saline, IR, Empty SPNP, and ATG7i-SPNP and scale bar = 20 μm for ATG7i-SPNP+IR long-term survivors) indicate positive staining for areas delineated in low-magnification panels. Representative images from a single experiment consisting of independent biological replicates are displayed.

Supplementary Table 3: Mouse and human ATG4b, ATG7, and ATG9b siRNA sequences.

siRNA	Company	Catalog #	Sequence
ATG4b (Mouse)	Origene	SR413163	rUrArGrCrCrArArUrArArArGrUrArGrUrGrGrGrCrArC rUrGrUrUrGrUrUrGrUrUrUrUrCrUrArCrUrGrArArArC rUrUrArUrUrUrArUrCrArGrArGrUrArUrCrArUrArUrG rUrCrArArArGrUrGrGrCrUrGrCrGrU
ATG7 (Mouse)	Origene	SR427399	rCrUrUrGrArUrCrArGrUrArCrGrArGrCrGrArGrArArG rGATrCrArUrCrArArGrGrGrCrUrArUrUrArCrUrArCrA rArUrGGTrGrCrUrCrUrGrArArCrUrCrArArUrArArUrA rArCrCrUrUGG
ATG9b (Mouse	Origene	SR421223	rCrArArUrGrArUrUrGrArArArArUrGrArGrArCrUrUrGr UrUrCrArA
ATG4b (Human)	Origene	SR323518	rArGrArUrGrGrArCrGrCrArGrCrUrArCrUrCrUrGrArC rCTArGrCrArUrUrGrArArGrArCrArUrArGrUrGrUrArU rUrUrCCTrGrUrCrCrArCrArUrUrGrCrArArUrGrGrAr CrArArCrArCTG
ATG7 (Human)	Origene	SR323157	rGrArGrUrCrArUrCrArGrUrGrGrArUrCrUrArArArUrC rUCArGrCrCrGrUrGrGrArArUrUrGrArUrGrGrUrArUr CrUrGrUTTrGrUrGrArArUrArUrCrArArArUrArCrCrAr ArUrCrUrUrAGA
ATG9b (Human)	Origene	SR317285	rCrCrUrGrGrArGrArUrUrArUrCrGrArCrUrUrUrUrUrU rCAT

Supplementary Table 3: Mouse and human ATG4b, ATG7, and ATG9b siRNA sequences. ATG4b, ATG7, and ATG9b mouse and human siRNA respective sequences, company origin, and catalog number.

Supplementary Table 4: Log-rank (Mantel-Cox) Kaplan Meier survival analysis of Figure 9d.

Group	MS Change	P value
Saline (MS: 33 DPI) vs. Empty-SPNP (MS: 35 DPI)	+ 2d	P = 0.0042
Saline (MS: 33 DPI) vs. IR (MS: 37 DPI)	+ 4d	P = 0.0653
Saline (MS: 33 DPI) vs. ATG7i-SPNP (MS: 26 DPI)	- 7d	P = 0.0242
Saline (MS: 33 DPI) vs. ATG7i-SPNP+IR (MS: 60 DPI)	+ 27d	P < 0.0001
Empty-SPNP (MS: 35 DPI) vs. IR (MS: 37 DPI)	+ 2d	P = 0.07025
Empty-SPNP (MS: 35 DPI) vs. ATG7i-SPNP (MS: 26 DPI)	- 9d	P = 0.0003
Empty-SPNP (MS: 35 DPI) vs. ATG7i-SPNP+IR (MS: 60 DPI)	+ 25d	P = 0.0001
IR (MS: 37 DPI) vs. ATG7i-SPNP (MS: 26 DPI)	- 11d	P = 0.0064
IR (MS: 37 DPI) vs. ATG7i-SPNP+IR (MS: 60 DPI)	+ 23d	P = 0.0003
ATG7i-SPNP (MS: 26 DPI) vs. ATG7i-SPNP+IR (MS: 60)	+ 34d	P < 0.0001

Supplementary Table 4: Log-rank (Mantel-Cox) Kaplan Meier survival analysis of Figure 9d. Detailed survival analysis using Log-rank (Mantel-Cox) Kaplan Meier test of animals implanted with genetically engineered mIDH1 glioma mouse cells treated with ATG7i-SPNP in combination with IR.